ADVANCED POSTBUCKLING AND IMPERFECTION SENSITIVITY OF THE ELASTIC-PLASTIC SHANLEY–HUTCHINSON MODEL COLUMN

Claus Dencker Christensen and Esben Byskov

ADVANCED POSTBUCKLING AND IMPERFECTION SENSITIVITY OF THE ELASTIC-PLASTIC SHANLEY–HUTCHINSON MODEL COLUMN

CLAUS DENCKER CHRISTENSEN AND ESBEN BYSKOV

The postbuckling behavior and imperfection sensitivity of the Shanley–Hutchinson plastic model column introduced by Hutchinson in 1973 are examined. The study covers the initial, buckled state and the advanced postbuckling regime of the geometrically perfect realization as well as its sensitivity to geometric imperfections.

In Section 1, which is concerned with the perfect structure, a new, simple explicit upper bound for all solutions to the problem is found when the tangent modulus at bifurcation vanishes compared to the linear elastic (unloading) modulus. The difference between the upper bound and the solution to an actual problem is determined by an asymptotic expansion involving hyperbolic trial functions (instead of polynomials) which fulfill general boundary conditions at bifurcation and infinity. The method provides an accurate estimate of the maximum load even if it occurs in an advanced postbuckling state. Finally, it is shown that the maximum load is often considerably larger than the bifurcation load.

Section 2 presents a new asymptotic expansion which is utilized to study the imperfection sensitivity of the Shanley–Hutchinson elastic-plastic model column. The method is mainly characterized by three novel features. Firstly, unlike other expansions which are performed around one or maybe two points, ours takes the total postbuckling path of the geometrically perfect structure as its basis, that is, the equilibrium of an imperfect path is written as the postbuckling path of the perfect structure plus an asymptotic contribution. Secondly, the expansion parameter is chosen as the buckling mode amplitude minus its value at initiation of elastic unloading. In this connection, the asymptotic expansion of initiating elastic unloading to the lowest order given by Hutchinson serves as a kind of boundary value for the asymptotic expression. Thirdly, a new and more suitable set of base functions is introduced to enhance the accuracy of the asymptotic expansion for large imperfection levels without compromising the asymptotic behavior for small imperfections. If an asymptotically exact postbuckling solution for the perfect structure around the maximum load has been obtained by some method, be it numerical or asymptotic, then the prediction of the imperfection sensitivity is asymptotically correct.

Introduction

Today, elastic-plastic stability of structures, including their imperfection sensitivity, may be examined by means of numerical methods. Such procedures may, however, suffer some major disadvantages. A complete analysis of the behavior of a perfect or a geometrically imperfect structure often becomes very time consuming, and in the vicinity of singularities, for example bifurcation, the equilibrium equations may become numerically unstable which might lead to divergence. This is one reason why analytical

investigation of stability problems is still important. Another, maybe even more important, ground for the interest in analytic methods is the desire to better understand elastic-plastic stability and imperfection sensitivity. It is therefore important to establish an analytic method for treatment of plastic stability.

For more than half a century, Koiter's general asymptotic theory of initial postbuckling and imperfection sensitivity of elastic structures has been available [Koiter 1945]. Development of a similar and as widely applicable theory of stability in the plastic range presents more difficulties, mainly due to the fact that, contrary to the case of elastic structures, the maximum load of a geometrically perfect elastic-plastic structure rarely occurs at bifurcation. To date, the most successful method has been established by Hutchinson [1973b]. However, as pointed out by Hutchinson himself, the method has a rather limited range of applicability for certain types of structures (see also [Hutchinson 1974]).

A short survey of plastic buckling.   The history of analytical treatment of elastic-plastic stability is only a little more than one hundred years old, beginning with the work of Engesser [1889], who proposed a formula for the plastic bifurcation load, later known as the *tangent modulus load*, of a column. His formula was subjected to criticism and Engesser derived another formula under the tacit assumption that bifurcation occurs under constant load, the so-called *reduced modulus load*. It appears that over the next 60 years almost any professor of structural mechanics had his own formula for plastic column buckling. In retrospect it seems clear that these formulas are just weighted averages of the two loads mentioned above, and sometimes the *Euler buckling load* is also included in the weighting. Based on experiments on aluminum columns and by analyzing the initial postbifurcation behavior of a simple model column, which we refer to as the *Shanley column*, Shanley [1947] showed that the tangent modulus load was indeed the most meaningful of the previously suggested plastic buckling loads and that at that load, bifurcation takes place under increasing load. Soon after, Duberg and Wilder [1952] introduced imperfections in the Shanley model column, and later Hill [1957] established the minimum energy criterion of stability for a rigid plastic body.

While the works mentioned above were mainly concerned with determination of the correct plastic bifurcation load and to some extent also with the initial postbifurcation behavior, analytic determination of the maximum load-carrying capacity of geometrically perfect and imperfect structures received much less attention. Not until the work by Hutchinson [1973b], and the survey article [Hutchinson 1974] was an asymptotic method in the spirit of Koiter established. Hutchinson introduced terms of fractional powers in the asymptotic expansion in order to handle elastic unloading. Hutchinson's method and ideas were further explored by, among others, Needleman and Tvergaard [1976] and van der Heijden [1979].

Hutchinson [1972; 1973a] and van der Heijden [1979] prescribe that elastic unloading initiates at bifurcation for the perfect structure. The point of initiating elastic unloading of the imperfect structure is determined by a simple one-term elastic asymptotic expansion. Hutchinson uses this point as basis for an asymptotic expansion similar to the one he suggested for the perfect structure, while van der Heijden also uses the point of initiating elastic unloading to construct solutions in the spirit of his perfect solution. Both these solutions tend to be considerably more complicated than their perfect counterparts but suffer the same shortcoming: relatively accurate estimates of the load-carrying capacity is only found when the maximum load occurs very close to bifurcation. This is, however, rarely the case in plastic stability problems. Note that neither of the solutions predicts asymptotically correct maximum loads for small imperfections.

Hutchinson and Budiansky [1976] discovered that when the critical load of an elastic-plastic structure coincides with the reduced modulus load the maximum loads in the presence of imperfections sometimes coincide with the maximum loads of the hypoelastic comparison structure, and a theory rather similar to the simpler elastic asymptotic Koiter theory yields exact asymptotic estimates of these maximum loads. Needleman and Tvergaard [1976] suggested that even when the maximum load of the imperfect structure is found after initiating elastic unloading a hypoelastic theory may still yield sufficiently precise results. They base their idea on the fact that the larger the imperfections the less significant elastic unloading becomes. Comparison with numerical results shows that when the equilibrium of the geometrically perfect structure is not significantly influenced by plasticity this method estimates the imperfection sensitivity extremely well, but when the added stiffness of the elastic unloading zone dominates postbuckling a hypoelastic theory cannot be used for accurate estimates.

Thus, when plasticity is included the imperfection sensitivity analysis becomes even more complex, partly because the maximum load of both the perfect and the imperfect structure may be far from bifurcation, and partly due to the fact that each equilibrium path of the imperfect structure has a singularity where elastic unloading initiates. Probably for these reasons it seems that very few new approaches to analytic treatment of plastic postbuckling and imperfection sensitivity have been proposed since the above mentioned studies and none appears to have led to much improvement over the existing methods. Thus, a simple and universally accurate method for handling imperfection sensitivity of plastic structures has not yet been established. In this connection it may be worth mentioning that Ming and Wenda [1990] postulated to have improved Hutchinson's asymptotic method by choosing a different perturbation parameter. However, a closer examination of their work reveals that they determine the asymptotic coefficients correctly, but that their asymptotic plots do not match these coefficients at all. The correct curves do not approximate the maximum load any better (or worse) than Hutchinson's did. The article by Scherzinger and Triantafyllidis [1998] is concerned with an asymptotic analysis of stability of elastic-plastic structures, but their expansion parameter ε describes the slenderness of the beams investigated rather than a displacement variable, as is the case in the present study.

Since the Sixties, great effort has been spent on nonlinear numerical investigations of more realistic elastic-plastic structures. In spite of their own merits, numerical investigations rarely lead to a deeper understanding of the phenomenon of elastic-plastic buckling, at least not unless a large number of computations are carried out.

Main objectives. The maximum loads, denoted $P_{\max}$, of the analytical methods mentioned above are all fairly well predicted when the maximum load occurs very close to the point of bifurcation, even though the matching buckling amplitude is sometimes rather poorly determined. When $P_{\max}$ lies far from the point of bifurcation the accuracy deteriorates rapidly. The main reason for including elastic unloading is the enhanced load-carrying capacity in postbuckling. Thus, an accurate determination of the postbuckling load reserve is of great importance, in particular when the maximum load becomes considerably higher than the bifurcation load.

In order to reduce the complexity of the problems as much as possible without loss of plastic characteristics, Hutchinson [1974] used a slightly modified version of the Shanley column which only differs from the original by being supported by a continuous row of springs and a nonlinear spring at the top in order to introduce various kinematic nonlinearities; see Figure 1. In the present paper we investigate both
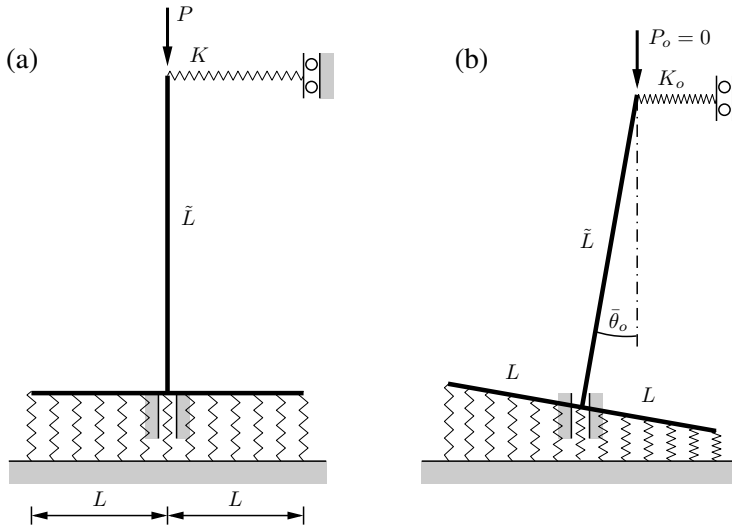
Figure 1. The continuous Shanley–Hutchinson column: (a) geometrically perfect; (b) geometrically imperfect.

the geometrically perfect and the geometrically imperfect version of the *Shanley–Hutchinson Column* and develop analytic methods which predicts the load-carrying capacity of the geometrically imperfect Shanley–Hutchinson elastic-plastic model column (see Figure 1(b), and for the the maximum load of its geometrically perfect counterpart, see Figure 1(a)) and concentrate on cases where $P_{\max}$ does not occur close to bifurcation.

The ultimate goal of the investigation of plastic stability is, of course, to allow plastic stability to be included in maximum load calculations for more realistic structures, but that is not within the scope of the present paper.

1. Geometrically perfect model column

1.1. *Preliminary analysis.* In order for a solution to the plastic postbuckling problem to be considered satisfactory, we require that its prediction of the maximum load be accurate compared to the postbuckling load reserve and that the results be stable in the sense that the solution should be valid for all relevant cases. Furthermore, it is important that the solution be relatively simple and straightforward to apply to real structures.

Before 1970 the models considered—for example, the original Shanley column—were so simple that it was possible to give explicit solutions, but with the continuous Shanley–Hutchinson column and other more realistic models the complexity of the solutions made this impossible. We emphasize that by an explicit solution we do not necessarily mean the exact equilibrium, rather *explicit* is used in the sense of an *approximation* which does not invoke incremental steps. By this definition Hutchinson's and van der Heijden's solutions are also explicit. Such explicit solutions are subject to some limitations with regard to generality which will also be present in this paper:

- No other singularity can be present after the bifurcation singularity and before maximum load (for example, mode interaction, extension of the unloading zone all the way through the cross-section, Bauschinger effects, etc.).

- Unloading must start at bifurcation, which it will do in most relevant stability cases; see, for example, [Hutchinson 1974], and certainly for the Shanley–Hutchinson column.

The first limitation can be overcome by splitting the solutions into parts between singularities. The latter problem rarely occurs because unloading usually starts at bifurcation.

Before we proceed the search for a solution valid far from bifurcation, we discuss the merits of the most important existing methods.

Hutchinson's asymptotic expansion. The asymptotic expansion for initial postbuckling in the plastic range due to Hutchinson [1974] is the foundation for later asymptotic approaches to plastic stability. It is the natural, albeit not as obvious, extension of the elastic asymptotic theory by Koiter [1945] except for the fact that fractional powers are present in the expansions. It accounts for elastic unloading and material nonlinearities, but is still, like its elastic counterpart, fairly straightforward to apply to structural problems. The disadvantage of the method and the reason that new analytic plastic methods are still interesting is that it furnishes rather crude estimates of the maximum load and its associated displacements, unless the maximum occurs very close to bifurcation. This fact was already pointed out by Hutchinson [1974]. Later, van der Heijden [1979] showed that expanding Hutchinson's method further often produces less accurate approximations of the maximum load due to the unpredictable range of convergence for ordinary asymptotic methods.

The reduced modulus solution by van der Heijden. In his study, van der Heijden [1979] recognized that it was not the behavior in the vicinity of bifurcation, but the behavior close to the maximum load that controls the imperfection sensitivity. This led him to give an asymptotic estimate of the possible maximum loads close to the reduced modulus load thereby gaining knowledge about the approximate asymptotic behavior at maximum load. He then matched the asymptotic expansion established by Hutchinson with his own and ended up with an approximate expression for the equilibrium from bifurcation to maximum load. For maximum loads close to bifurcation this yields excellent predictions, but further away from bifurcation the accuracy decreases considerably, yet slightly less than Hutchinson's, as it appears from van der Heijden's comparison with numerical results [van der Heijden 1979]. The implementation of van der Heijden's method is lengthy in that three asymptotic expansions must be established, and the matching procedure is not straightforward and therefore hard to extend to higher degrees of asymptotic expansions as well as to generalize to other kinds of structures.

The hypoelastic imperfection sensitivity studies by Hutchinson and Budiansky and by Tvergaard and Needleman. The hypoelastic approach used by Hutchinson and Budiansky [1976] and by Needleman and Tvergaard [1976] suppresses the elastic unloading branch making it possible to analyze a nonlinear comparison version of plastic structures asymptotically in the spirit of Koiter's well-known linear elastic approach [Koiter 1945]. However, the similarity between the plastic structure and its associated comparison model in postbuckling strongly depends on the extent of the unloading zone and its added stiffness. This approximation will therefore only be satisfactory when elastic unloading is of minor importance.

Parameters of the solution. The postbuckling solution depends on the parameters of the material non-linearity represented in the stress-strain relation and on the parameters of the kinematic nonlinearity concentrated in the nonlinear spring at the top of the column; see Figure 1(a). To fully understand the plastic behavior in postbuckling of the column, it is therefore crucial to investigate the influence the parameters of the model on the location of the maximum load point.

As presupposed in Section 1.2 the column unloads linearly elastic with a constant Young's modulus E. The larger E, the more elastic unloading dominates and makes the maximum load move away from bifurcation. The basic expressions (9) and (10) do not depend on the shape of the stress-strain relation before bifurcation, only on the values of E and E_t, where E_t denotes the tangent modulus, which, in general, depends on the strain.

As in most other buckling and postbuckling studies we assume that the tangent modulus E_t decreases with strain and approaches zero at infinite strain. The smaller the rate of decrease of E_t, the further from bifurcation the maximum load is.

The spring K (see Figure 1(a)) provides a *destabilizing* nonlinearity in order to make the structure *imperfection sensitive* and ensure the existence of a maximum load after bifurcation. The smaller the rate of increase of the kinematic nonlinearity the further from bifurcation the maximum load is going to be.

The stress-strain relation is mainly important close to bifurcation because, as E_t approaches zero, K will totally dominate the equilibrium equations. Since it is known that existing methods work well close to bifurcation it is particularly interesting to examine the behavior as the locus of maximum moves away from the point of bifurcation. This means that an investigation where K as well as the rate of decrease in E_t is small, while E is large, is particularly relevant to perform. For the sake of studying plastic effects on stability it is especially important that accurate results are obtained when E_t^c/E is small, where E_t^c designates the value of E_t at bifurcation.

We shall try not to exploit features that are particular to the Shanley–Hutchinson-model in our derivations in the hope that the method developed here is applicable to a broader variety of structures.

General idea. It is evident from the above that when examining plastic postbuckling behavior, one has to include elastic unloading. To keep it simple and straightforward, we would like to avoid the complications and limitations inherent in the reduced modulus approach, yet we would like to utilize the knowledge about the equilibrium when far from bifurcation in order to determine maxima in the advanced postbuckling regime. Hutchinson's general, simple and excellent concept of a Koiter-like asymptotic expansion [Hutchinson 1974] does not cover advanced postbuckling states due to the fact that the postbuckling fields were expanded in (fractional) powers of the buckling mode amplitude. Therefore, focus was centered on the immediate neighborhood of bifurcation. It is a well-known fact that the range over which an asymptotic expansion yields sufficiently accurate results is hard to predict, in fact, the range can be extremely small and may very well decrease with the number of terms in the asymptotic expansion, but choosing a set of more suitable trial functions, if available, may improve convergence. Below, we show that use of other trial functions that behave in a globally correct way may indeed extend the validity to cover advanced postbuckling states.

In order to improve the approximation of the correct equilibrium by the asymptotic expansion suggested by Hutchinson [1973b; 1974] and thereby obtain reliable results even when the maximum supported load does not appear close to bifurcation, we shall first examine carefully the general behavior of the Shanley–Hutchinson column in advanced postbuckling. Subsequently, we will use the acquired knowledge to choose suitable trial functions and make an asymptotic match at bifurcation between the new expansion and the original one by Hutchinson.

1.2. Basic equations. Throughout this paper a superscript ^{c} or a subscript $_c$ denotes a value taken at bifurcation. Superscript ^{o} or subscript $_o$ refers to Hutchinson's original values with dimensions, while nondimensional quantities are left unmarked for convenience.

In order to isolate the kinematic nonlinearities in the top spring shown in Figure 1(a), Hutchinson used the approximation $\sin(\theta) \approx \theta$, and gave the top spring response as

$$K_o(\theta_o) = k_{io}\theta_o^{i+1}, \quad i \in \{1, 2, 3, \ldots\} \tag{1}$$

where we note that *positive* values of k_{io} imply *destabilizing*. Since the lowest power of θ_o is 2, asymmetric postbifurcation of the kind experienced by the so-called Roorda Frame is not covered; see [Roorda 1965] and [Koiter 1966] for the elastic version, and [Byskov 1982–83] for the elastic-plastic version. In the purely elastic case, symmetric postbuckling like the one typical of many shell structures may be modeled by letting $k_{1o} > 0$. In the following examples we do not cover the case $k_{2o} \neq 0$ because it is rather trivial, but, as we shall see, for a special reason, address the one with $k_{3o} > 0$.

Together, Figure 1(a) and Figure 2 define the geometry. Note that the quantity E_{eff}, which is introduced below, designates the immediate effective tangent modulus, that is, it is E_t for loading and E for unloading, and that s is the stress. We keep as close to Hutchinson's original notation as possible, but introduce the following nondimensional quantities:

$$
\begin{aligned}
x &= \frac{x_o}{L} & P &= \frac{P_o}{P_o^c} & s &= \frac{s_o}{2s_o^c} \\
\theta &= \frac{\tilde{L}}{L}\theta_o & u &= \frac{\tilde{L}}{L^2}u_o & \varepsilon &= \frac{\tilde{L}}{L^2}\varepsilon_o \\
E_{\text{eff}} &= \frac{3E_{\text{eff}}^o}{2E_{to}^c} & k_i &= \frac{L^{i+2}}{P_o^c\tilde{L}^i}k_{io} & \bar{\theta} &= \frac{\tilde{L}}{L}\bar{\theta}_o
\end{aligned}
\tag{2}
$$

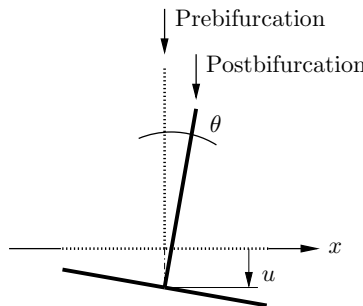**Figure 2.** Definition of the kinematic variables u and θ.

where $\bar{\theta}$ signifies a geometric imperfection; see Section 2.1, Figure 10.

The lowest bifurcation load is given by Hutchinson as

$$P_o^c = \frac{2E_{to}^c L^3}{3\tilde{L}},$$

which, by the way, is the same as the bifurcation load of the nonlinear elastic comparison model. The following nondimensional quantities evaluated at bifurcation are used extensively in the following:

$$P_c = 1, \qquad s_c = \frac{1}{2}, \qquad E_t^c = \frac{3}{2}. \tag{3}$$

Utilize the nondimensional quantities introduced in Equation (2) to obtain the nondimensional equilibrium equations of the geometrically perfect realization of the model column:

$$P = \int_{-1}^{1} s\,dx, \qquad P(\theta) + K(\theta) = \int_{-1}^{1} sx\,dx, \tag{4}$$

where, in analogy with Equation (1), the nondimensional spring stiffness is

$$K(\theta) = k_i \theta^{i+1}, \quad i \in \{1, 2, 3, \ldots\},$$

and the strain-displacement relation of the continuous spring support is

$$\varepsilon = u + \theta x. \tag{5}$$

When linear-elastic unloading is included, the stress increment $\dot{s}$ is given as

$$\dot{s} = E_{\text{eff}}\,\dot{\varepsilon}, \tag{6}$$

where

$$E_{\text{eff}} = \begin{cases} E_t(\varepsilon), & \text{for} \quad \big((s = s_{\max}) \wedge (\dot{s} \geq 0)\big), \\ E, & \text{for} \quad \big((s < s_{\max}) \vee \big((s = s_{\max}) \wedge (\dot{s} < 0)\big)\big), \end{cases} \tag{7}$$

and where a dot indicates an increment, and $s > 0$ implies compression.

The incremental equilibrium equations are readily obtained by differentiation of Equation (4) and the use of Equation (6).

The zone of elastic unloading spreads from the edge of the column support and extends to the point d, where no sign reversal of the strain rate has occurred, that is, $\partial \varepsilon / \partial \theta = \partial u / \partial \theta + d = 0$, and thus

$$d = -\frac{\partial u}{\partial \theta}. \tag{8}$$

When $d < -1$, there is no elastic unloading. Elastic unloading always initiates at the lowest bifurcation load of the perfect Shanley–Hutchinson column [Hutchinson 1974]. After introduction of the constitutive equation (7) the incremental equilibrium equations of the geometrically perfect model column may be written:

$$\frac{\partial P}{\partial \theta} = \int_{-1}^{d} E\left(\frac{\partial u}{\partial \theta} + x\right) dx + \int_{d}^{1} E_t\left(\frac{\partial u}{\partial \theta} + x\right) dx \tag{9}$$

and

$$\frac{\partial P}{\partial \theta} \theta + P + \frac{\partial K}{\partial \theta} = \int_{-1}^{d} E\left(\frac{\partial u}{\partial \theta} + x\right) x dx + \int_{d}^{1} E_t\left(\frac{\partial u}{\partial \theta} + x\right) x dx. \tag{10}$$

1.3. *General behavior of the equilibrium.* Before the postbuckling equations (9) and (10) can be solved, the constitutive relation, given by E and the expression for $E_t(\varepsilon)$ after buckling, as well as the kinematic nonlinearity in terms of $K(\theta)$ must be chosen. The study of plastic postbuckling mainly differs from the elastic in that, in the plastic case it is necessary to consider the effect of stiffening by unloading with the modulus E. In order to examine the influence of the stiffening, we therefore keep the postbuckling up-loading stress-strain relationship and the kinematic nonlinearities fixed only allowing the initial Young's modulus E to vary. An upper bound for the equilibrium is found when the unloading modulus approaches infinity, that is, when $E_t^c/E = 0$. When the initial slope of the postbuckling equilibrium is negative, that is, when $(\partial P/\partial \theta)_c \leq 0$, a lower bound with P_c as the maximum is characterized by $E_t^c/E = 1$. After the bounds have been established we are furnished with a firm frame for our further investigations: all other solutions are limited to this area and are furthermore not allowed to cross each other.

Upper bound. When $E \to \infty \Rightarrow E_t^c/E \to 0$ and it is assumed that $|P| < \infty$ and $|\partial P/\partial \theta| < \infty$, Equations (9) and (10) simplify substantially in that the introduction of $E_t^c/E = 0$ provides

$$0 = \int_{-1}^{d} \left(\frac{\partial u_\infty}{\partial \theta} + x\right) dx \qquad \text{and} \qquad 0 = \int_{-1}^{d} \left(\frac{\partial u_\infty}{\partial \theta} + x\right) x dx. \tag{11}$$

Superscript ∞ or subscript ∞ denotes the upper bound. Insert d given by Equation (8) to solve (11). The only possible solution is

$$\frac{\partial u_\infty}{\partial \theta} = 1 \qquad \Longrightarrow \qquad u_\infty = \theta + u_c, \tag{12}$$

which means that the unloading zone does not progress into the cross-section, but is limited to one edge of the support. Express E by P and u in Equation (9) as

$$E = \frac{\frac{\partial P}{\partial \theta} - \int_{d}^{1} E_t\left(\frac{\partial u}{\partial \theta} + x\right) dx}{\int_{-1}^{d} \left(\frac{\partial u}{\partial \theta} + x\right) dx},$$

and insert this expression and Equation (12) in Equation (10) to determine the load $P^\infty(\theta)$ associated with the upper bound

$$(1+\theta)\frac{\partial P^\infty}{\partial \theta} + P^\infty = \int_{-1}^{1} E_t(x+1)^2 dx - \frac{\partial K}{\partial \theta},$$

identified as a first order linear differential equation, which, when the boundary condition $P^\infty(0) = 1$ is applied, has the solution

$$P^\infty(\theta) = \frac{1}{1+\theta}\left(-K(\theta) + \int_{-1}^{1} s_{\text{hypo}}(x+1) dx\right). \tag{13}$$

Here, s_{hypo} is the nondimensional nonlinear hypoelastic postbuckling stress found independent of elastic unloading. For some choices of constitutive relations the integral may be computed explicitly when the stress-strain relationship is chosen.

The upper bound solution is particularly interesting because it covers the solutions where the maximum load appears as far from bifurcation as possible. This provides an ideal basis for the selection and fitting of asymptotic trial functions which provide reliable solutions far from bifurcation.

Lower bound. When E_t, as supposed, is a decreasing function of ε, the plastic model is able to carry higher loads than the related hypoelastic comparison model because of the stiffening of the elastically unloaded region. Thus, the comparison model provides an absolute lower bound for the plastic solutions. As mentioned above, in the plastic regime the maximum load usually does not occur at bifurcation. It is the case under the usual conditions that the stress-strain relation is continuous and that E is larger than E_t^c, otherwise the structure will not feel unloading as a stiffening. Furthermore, it is assumed that bifurcation does not take place at a sharp bend in the stress-strain relation. If, as an experiment, we choose $E_t^c/E \geq 1$ in the buckling model the usual conditions mentioned above are violated and it may be realized that the initial postbuckling stiffness will be smaller than that of the comparison model. The value of $\partial P_c/\partial \theta$ of the comparison model is always smaller than or equal to zero when no stabilizing kinematic nonlinearities are present and therefore the plastic model with $E_t^c/E = 1$ has a maximum at bifurcation. From this we deduce the important information that, as E_t^c/E decreases from 1 to 0, the maximum load will move from the bifurcation point to the maximum of P^∞ given by Equation (13). Since s is monotonically increasing from $x = -1$ to $x = 1$ for $\theta > 0$, the right side of Equation (4) will always be positive. This provides an absolute minimum for the solution of Equation (4) (right) and therefore a lower bound for any plastic solution with $E_t^c/E < 1$:

$$P \geq \frac{-K(\theta)}{\theta} = P_{\text{lower}}. \tag{14}$$

1.4. *Hyperbolic asymptotic method.* It may be shown that, as θ approaches infinity and E_t approaches zero, the integral in the upper bound solution Equation (13) loses significance compared to $K(\theta)$ yielding the far field solution

$$\lim_{\theta \to \infty} P^\infty \to \begin{cases} 0, & K(\theta) = 0, \\ -\dfrac{K(\theta)}{1+\theta}, & K(\theta) \neq 0. \end{cases}$$

Compare the above equation to the absolute minimum solution Equation (14) and notice that they are approximately parallel to each other with a limited distance less than 1 when θ is large. Furthermore, we find that the solutions are asymptotically similar, that is, $P^\infty \sim P_{\text{lower}}$ for $\theta \to \infty$. Any arbitrary solution lies between the upper and lower bound and must therefore also behave asymptotically like the upper bound at infinity with a distance less than 1. In order to use the knowledge of the upper bound and the relative shape of other solutions it seems obvious to concentrate on an asymptotic expansion of the difference $\Delta P^\infty \leq 0$ between the upper bound P^∞ and the solution P; see Figure 3.

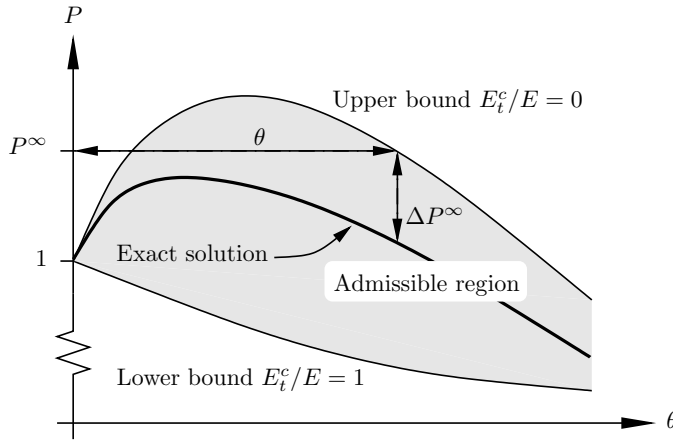$$\Delta P^\infty = P - P^\infty. \tag{15}$$

Figure 3. The hyperbolic asymptotic method and the admissible region.

This choice has the convenient feature that it predicts both the maximum load and its associated displacement well when the solution lies close to the upper bound, even when the maximum load occurs far from bifurcation. The usual polynomial asymptotic trial functions are, however, not suited for the expansion of ΔP^∞ because they do not in general fulfill the above-mentioned conditions of parallelism and negativity. Hyperbolic functions[1] not only satisfy these conditions, but have the property that their lowest order terms dominate the general behavior, that is, not only for small, but for all values of θ. The basic idea is to establish an hyperbolic approximation $\mathcal{H}(\theta)$ using the characteristics of ΔP^∞ and matching these terms with the first few nonvanishing asymptotic terms of the series of Hutchinson [1974]; see Appendices A and B. Since ΔP^∞ in general only vanishes *relative* to P^∞ at infinity, we choose the leading power of the denominator to be only fractionally higher than that of the numerator. The lowest order asymptotic term is then given by the numerator, while the next terms are used in the denominator to restrain the growth of the expression. In practice, applying the first two terms of the denominator proves to furnish a sufficiently accurate first approximation

$$\Delta P^\infty \approx \mathcal{H}(\theta) = a_1^\infty H(\theta) = a_1^\infty \frac{\theta^{\frac{3}{2}}}{(1 + h_1 \theta^{\frac{1}{2}} + h_2 \theta)^2}.$$

Notice that $\mathcal{H}(\theta)$ will always be negative because, according to Equation (B.3); see Appendix B, and the above equation, $a_1^\infty = a_2^\Delta < 0$. If further exploration is desired, $H(\theta)$ provides a basic trial function for a *hyperbolic* asymptotic method

$$\Delta P^\infty = a_1^\infty H(\theta) + a_\alpha^\infty H(\theta)^\alpha + a_\beta^\infty H(\theta)^\beta + O(H(\theta)^\gamma), \quad 1 < \alpha < \beta < \dots < \gamma. \tag{16}$$

When $H(\theta)$ is chosen to match the first three nonvanishing asymptotic terms, a_α^∞ and α may be determined from the fourth term and so forth. The general expansion Equation (16) still behaves globally correct. It approaches zero at infinity and higher order asymptotic terms of $H(\theta)$ become increasingly less significant compared to lower order terms for large values of θ.

---

[1]Here, we use the term *hyperbolic* in a somewhat generalized sense.

Hyperbolic asymptotic expansion coefficients. In order to determine a_1^∞, h_1, h_2, a_α^∞, α, etc., we match the hyperbolic expansion Equation (16) with that of Hutchinson [1974]. An asymptotic expansion carried to a higher degree in θ than Hutchinson's is given in Appendix A; see Equations (A.1), (A.2), (A.6) and (A.7). The extension of the method is straightforward, but rather lengthy. The polynomial expansion of $H(\theta)$ is

$$H(\theta) = \theta^{\frac{3}{2}} - 2h_1\theta^2 - (2h_2 - 3h_1^2)\theta^{\frac{5}{2}} + (6h_1h_2 - 4h_1^3)\theta^3 + O(\theta^{\frac{7}{2}}).$$

Insert the above equation into (16) and compare with Equation (B.2) to obtain expressions for the hyperbolic coefficients

$$a_1^\infty = a_2^\Delta, \qquad h_1 = \frac{a_3^\Delta}{-2a_2^\Delta}, \qquad h_2 = \frac{a_4^\Delta}{-2a_2^\Delta} + \tfrac{3}{2}h_1^2,$$

where a_i^Δ are the polynomial asymptotic coefficients given in Equation (B.3). When a_1^∞, h_1 and h_2 are determined from the three initial asymptotic terms, α must be equal to 2 for the θ^3-term to match. Thus,

$$\alpha = 2: \qquad a_\alpha^\infty = a_2^\infty = a_5^\Delta - a_2^\Delta(6h_1h_2 - 4h_1^3).$$

Although we have found no case where it was necessary to determine the β-term of Equation (16), we mention that the value of β is $\tfrac{7}{3}$. Carrying out the expansion to cover this is, however, so lengthy and complicated that it may not be worth the while.

Finally, inserting Equation (16) into (15) provides the total solution for P.

The fact that we have chosen other trial functions than the usual polynomials does not change the asymptotic behavior of the initial postbuckling path, that is, for small values of θ. The new asymptotic expansion will therefore be no worse than the original one when E_t^c/E is increased and the maximum load approaches bifurcation as shown in the lower bound solution. This indicates that the use of our hyperbolic trial functions will produce accurate maximum loads for all $0 \le E_t^c/E \le 1$. When P is determined, the displacement u may be found after P has been inserted into Equations (9) and (10).

1.5. *Constitutive relation.* Traditionally, a Ramberg-Osgood type stress-strain relation has often been employed in elastic-plastic buckling studies, such as the important ones by Hutchinson [1974] and by van der Heijden [1979]. For our purpose, this constitutive model has the disadvantage of expressing the strain in terms of the stresses instead of the other way around implying numerical integrations. As far as possible, we prefer analytic manipulations and therefore propose another constitutive model, which provides an explicit formula for the tangent modulus E_t in terms of the added strain $\Delta\varepsilon$ after bifurcation and a shape parameter ρ:

$$E_t = \frac{E_t^c}{1 + \rho\Delta\varepsilon} = \frac{3}{2(1 + \rho\Delta\varepsilon)}. \tag{17}$$

When ρ and the ratio E_t^c/E are varied, this relation may cover a wide variety of constitutive behavior and may be considered as versatile and valid as the Ramberg-Osgood type formula [Hutchinson 1974]:

$$\frac{\varepsilon}{\varepsilon_y} = \frac{s}{s_y} + \psi\left(\frac{s}{s_y}\right)^n, \tag{18}$$

where ε_y and $s_y = E\varepsilon_y$ are effective initial yield values, n is the hardening parameter, and ψ is a shape parameter.

In Example 1 below we wish to compare results obtained by our improved method with those found by Hutchinson [1974] and by van der Heijden [1979]. Therefore, we need to examine the differences between the two constitutive relations for a certain set of parameters. Both Hutchinson [1974] and van der Heijden [1979] take $(n, \psi) = (3, 0.2)$. Numerical experiments show that the tangent modulus decrease rate $\rho = 3.0$ in Equation (17) produces a constitutive law very similar to the one used by Hutchinson and van der Heijden; see Figure 4, where the relative difference between the values of the tangent modulus E_t found by the two constitutive relations is plotted over a very large interval of $\Delta\varepsilon$. It may be worthwhile noticing that for $n = 10$ the proper value of ρ is about 25.

Stress-strain relation and the upper bound. In Equation (13) the postbuckling stress-strain relation is represented by s_{hypo}. To avoid a numerical calculation of the integral, we therefore chose E_t as an explicit function of ε; see (17). Now, (17) may yield the following expression for s_{hypo}:

$$s_{\text{hypo}} = \frac{E_t^c}{\rho} \ln(1 + \rho\Delta\varepsilon) + \frac{1}{2} = \frac{3}{2\rho} \ln(1 + \rho\Delta\varepsilon) + \frac{1}{2}. \tag{19}$$

At the upper bound, straightforward use of Equation (12) provides $\Delta\varepsilon = (1 + x)\theta$. Introduce this expression into (19) and exploit this in Equation (13) to get an explicit nondimensional expression for the upper bound:

$$P^\infty = 1 + \frac{1}{1 + \theta} \left[-\theta - K(\theta) + \frac{3}{2\rho} \left(\frac{1}{\rho\theta} - 1 + \left(2 - \frac{1}{2(\rho\theta)^2} \right) \ln(1 + 2\rho\theta) \right) \right]. \tag{20}$$

Example 1: comparison with previous results. As a demonstration of the improved accuracy of our new method, we compare the postbifurcation equilibrium with the asymptotic solution of Hutchinson [1974] and with the approximate solution by van der Heijden [1979] and utilize numerical results to judge the accuracy for a case which was found to be particularly demanding by Hutchinson [1974] and van der Heijden [1979], namely the case where $E_t^c/E = 0.459$. Furthermore, the example covers cases where the maximum load occurs close to bifurcation and where it lies close to the upper bound maximum.
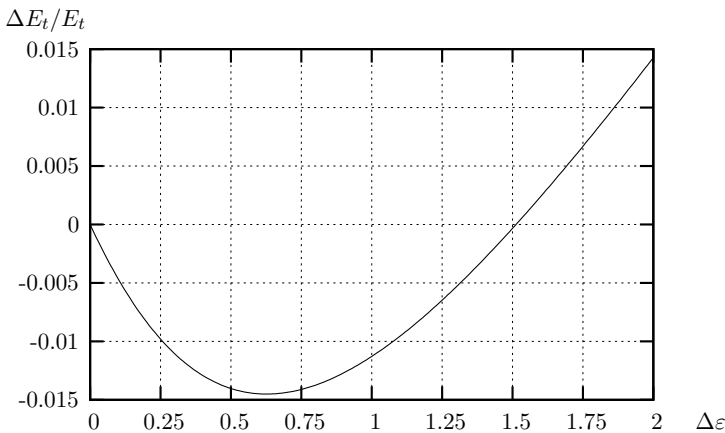

Figure 4. Relative difference between E_t found by the Ramberg-Osgood constitutive law Equation (18) with $(n, \psi) = (3, 0.2)$ and by Equation (17) with $\rho = 3$.
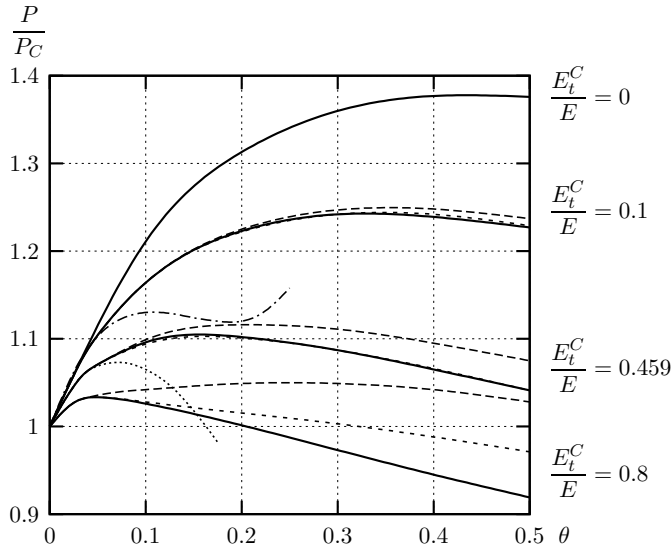
Figure 5. Postbuckling equilibria of the hyperbolic asymptotic method compared with numerical results, $(n, \psi) = (3, 0.2)$, $\rho = 3.0$, $k_i = 0$. Hutchinson's and van der Heijden's results are only plotted for $E_t^c/E = 0.459$. Here, the dotted line shows Hutchinson 1973, dot-dashed line, van der Heijden 1979, thin dashed line, 2 Hyperbolic terms, thick dashed line, 1 Hyperbolic term and solid line, Numerical.

Figure 5 contains plots of the postbuckling path determined by our hyperbolic asymptotic solution with 1 and 2 terms and by numerical computations, respectively. For purpose of comparison, the upper bound solution $E_t^c/E = 0$ is also indicated.

A good measure of the effect of some hyperbolic asymptotic term, $cH(\theta)^k$, on the solution is its maximum value. In each example, define $\widetilde{H}$ such that its maximum value is 1. Then, the hyperbolic asymptotic expressions (15) and (16) yield:

$$\frac{E_t^c}{E} = 0.1: \qquad P = P^\infty - 0.16\widetilde{H} - 0.01\widetilde{H}^2, \quad \widetilde{H} \equiv \frac{17.2\theta^{\frac{3}{2}}}{(1 + 0.13\theta^{\frac{1}{2}} + 3.01\theta)^2},$$

$$\frac{E_t^c}{E} = 0.459: \qquad P = P^\infty - 0.33\widetilde{H} - 0.04\widetilde{H}^2, \quad \widetilde{H} \equiv \frac{22.5\theta^{\frac{3}{2}}}{(1 + 0.35\theta^{\frac{1}{2}} + 3.39\theta)^2}, \qquad (21)$$

$$\frac{E_t^c}{E} = 0.8: \qquad P = P^\infty - 0.36\widetilde{H} - 0.06\widetilde{H}^2, \quad \widetilde{H} \equiv \frac{45.0\theta^{\frac{3}{2}}}{(1 + 0.75\theta^{\frac{1}{2}} + 5.00\theta)^2}.$$

Notice that the maximum (coefficient) value of the second asymptotic term is small compared to the maximum of the first asymptotic term even when E_t^c/E is much greater than 0 and the solution lies far from the upper bound. This indicates that the solution is relatively accurate even with only one asymptotic term. Still, the ratio between the first and the second asymptotic coefficient does not drop

significantly for increasing ratios of E_t^c/E, which indicates that more than one asymptotic term is needed for satisfactory results when the solution lies far from the upper bound.

From Figure 5, it is clear that the one-term hyperbolic solution provides excellent agreement with the numerical results when E_t^c/E is small. As E_t^c/E is increased and the solution moves away from the upper bound, the accuracy becomes less good. Employment of a second hyperbolic term makes the hyperbolic solution almost identical to the numerical one for $\theta \lesssim \theta_{\max}^\infty \approx 0.46$ both when $E_t^c/E = 0.1$ and $E_t^c/E = 0.459$. For $E_t^c/E = 0.8$ the maximum load and its neighborhood are determined accurately because of their proximity to bifurcation, but the solution is so far from the upper bound that the general hyperbolic asymptotic postbuckling path starts to deviate from the numerical one from $\theta \approx 0.1$. This is in agreement with what was deduced from Equation (21).

As expected, the two-term hyperbolic solution is considerably closer to the general numerical equilibrium than Hutchinson's and van der Heijden's solutions for $E_t^c/E = 0.459$ and the maximum load is more precise. Both Hutchinson's and van der Heijden's methods are basically polynomial asymptotics emanating from the ordinate axis, and therefore their solutions tend to deteriorate rapidly with increasing θ. Of the solutions investigated by Hutchinson and by van der Heijden, the case with $E_t^c/E = 0.459$, $k_i = 0$ exhibits the greatest ratio between the maximum load and the critical load and the largest θ-value at maximum load. From Figure 5 it is seen that other equilibria have maxima that occur significantly further from the bifurcation point and it is for such cases the hyperbolic method has its real *raison d'être*.

Even though the maximum load is determined with excellent accuracy by a two-term hyperbolic expansion, the value of θ at maximum may not be as precise.

Example 2: maximum loads. As stated earlier, our real interest lies in a precise determination of the maximum load. Previously, we have discussed the impact of the different parameters of the model on the location of maximum load relative to the critical load. The implementation of the postbuckling uploading stress-strain relation Equation (19) reduces the number of independent parameters in the determination of $P_\infty(\theta)$ to the kinematic nonlinearities, k_i, the rate of decrease in tangent modulus ρ and the level of plasticity E_t^c/E.

The parameters, k_i, control the fundamental *overall* shape of the equilibrium. Three basically different shapes may be distinguished:

(i) $k_i = 0$: no destabilizing kinematic nonlinearity is present. The maximum load will be far from bifurcation.

(ii) $k_1 \neq 0$: a rapid initial drop in load-carrying capacity will occur and the maximum load is close to bifurcation.

(iii) $k_i \neq 0$, i large: if i is sufficiently large the k_i-term will not be felt at the present stage of Hutchinson's asymptotic expansion Equation (B.2). The third spring constant, k_3, is the lowest level of kinematic nonlinearity not to appear in the terms of the Hutchinson asymptotic expansion used to determine the first 2 hyperbolic asymptotic terms. On the other hand, in the application of our method it enters through the expression (20) for P^∞. To have any noticeable influence on the maximum load, k_3 must be relatively large. When $\theta = 0.5$, the value $k_3 = 12$ furnishes a kinematic nonlinearity equal the nonlinearity associated with $k_1 = 3$.
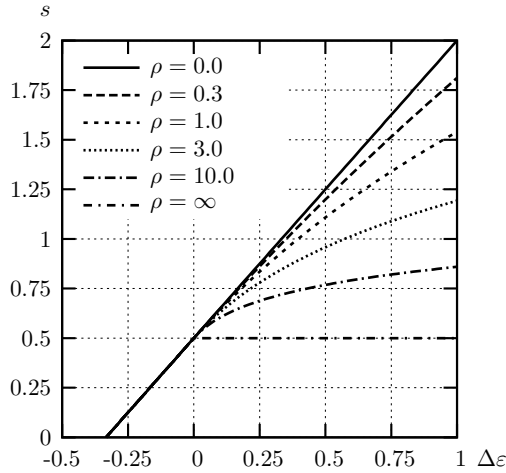
Figure 6. Stress-strain relations for ρ-values used in the maximum load plots. Unloading paths are not shown.

Figures 7, 8 and 9 show the maximum load for each of these cases as a function of the level of plasticity E_t^c/E for the tangent modulus decrease rate, ρ, varying between no decrease $\rho = 0$ and infinitely rapid decrease $\rho \to \infty$, as illustrated in Figure 6. As is clear from the figure, a wide spectrum of stress-strain relations are covered by the constitutive equation Equation (17).

Because of the different nature of each of the plots in Figures 7–9, we shall first examine each plot separately and then draw a more general conclusion. Note that, in order to make it possible to differentiate between the curves found by the hyperbolic method and by numerical computations, the plots in Figures 7–9 are scaled differently.
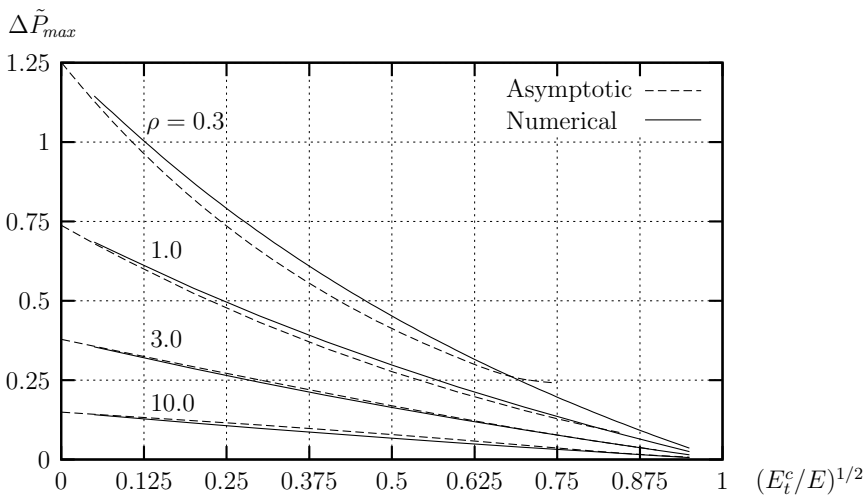

Figure 7. Maximum loads approximated with 2 asymptotic terms, $K(\theta) = 0$.
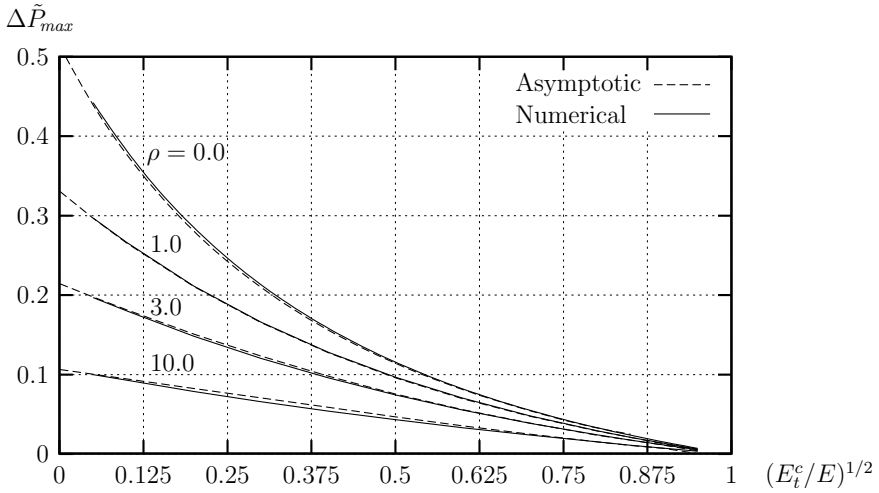
Figure 8. Maximum loads approximated with 2 asymptotic terms, $K(\theta) = 3\theta^2$.

- Figure 7, $k_i = 0$: In this case, the kinematic nonlinearity is as weak as possible in that the only kinematically nonlinear effect is the one which provides bifurcation. Therefore, the maximum load curve for $\rho = 0.0$ does not exist for finite θ. This means that when ρ is close to 0, the 2-term hyperbolic expansion does not provide a maximum because it is too far from both the upper bound and bifurcation.

  Apart from the above-mentioned exception, the *added* load-carrying capacity in postbuckling, ΔP_{max}, is found with only a small relative error of less than $\approx 10\%$ everywhere.

  The plot shows that ΔP_{max} is often significant compared to P_c as it for $\rho \leq 0.3$ becomes as large as 125% of P_c (recall that $P_c = 1$). For $\rho \to 0$ the upper bound solution yields a ΔP_{max} of 400% of P_c.

- Figure 8, $k_1 = 3$: Here, the kinematic nonlinearity is strong and, as a consequence of this, all maximum loads are extremely well approximated independently of the distance from the bifurcation point. This hinges on the fact that every solution is close to both the upper bound and the bifurcation point at maximum. Observe that, even when the first order kinematic nonlinearity, $k_1 = 3$, is large, the column has a considerable load-carrying reserve in postbuckling of up to $\approx 50\%$ of P_c when ρ and E_t^c/E are small.

- Figure 9, $k_3 = 12$: As mentioned above, this is a case where k_i only enters through the formula for ΔP^∞. Therefore, the approximations by the hyperbolic expansion could be expected to be inaccurate.

  However, except for fairly large values of E_t^c/E and small values of ρ, the difference between the predictions of the hyperbolic expansion and those obtained by numerical computations is small. Though not as precise as in the above cases, the hyperbolic expansion curves still yield satisfactory accuracy, generally under 15% relative error on the postbuckling load reserve, except very close to linear elastic, kinematically linear behavior.
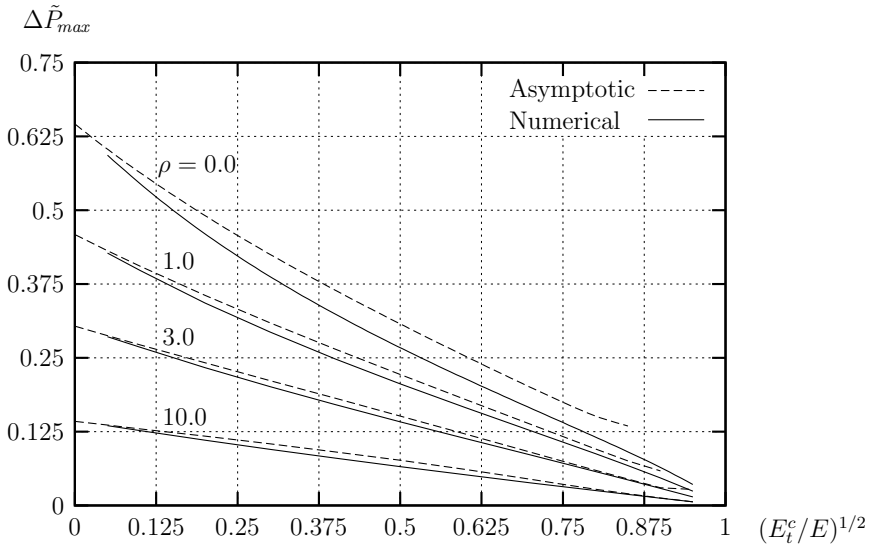
Figure 9. Maximum loads approximated with 2 asymptotic terms, $K(\theta) = 12\theta^4$.

In this case, the Hutchinson asymptotic expansion is here identical to the expansion for $k_i = 0$. For ρ large the maximum loads are almost not influenced by the kinematic nonlinearity and they equal the loads for $k_i = 0$ in Figure 7.

Our method has thus proved to be capable of handling effects that are not included in the Hutchinson asymptotic expansion, simply because of the influence from ΔP^∞.

We emphasize that the precision of the postbuckling load reserves determined by the hyperbolic asymptotic method is generally satisfactory when 2 terms are used. Only very close to linear elasticity combined with no dominating destabilizing kinematic nonlinearities (where the postbuckling load reserve is insignificant) may a third term be necessary to ensure sufficient accuracy.

From our plots we conclude that the model column is often able to carry loads which are much larger than the critical load, even without kinematically stabilizing effects in postbuckling. It is therefore important to have an accurate method for advanced postbuckling calculations, and the hyperbolic asymptotic method is found to fulfill this demand.

It may be argued that some of the large maximum loads are found at extreme values of the angle θ that would never be allowed in a design situation. Yet those loads are interesting because the maximum load-carrying capability will serve as an energy absorber of extreme unpredicted influences or imperfections and thereby prevent sudden collapse of stability. Also, since we are not studying a real structure, but a model column, the values of θ must not be taken too literally.

Conclusion. A hyperbolic asymptotic method for initial as well as advanced postbuckling analysis of Hutchinson's plastic model column is derived. The simple explicit solution for $E_t^c/E = 0$ (the upper bound) is found and it is shown that any other solution must approach it asymptotically to lowest order at infinity. The difference between the upper bound and the actual solution is estimated by an asymptotic expansion with hyperbolic trial functions that vanish at infinity.

It is shown that maximum loads are often obtained far from bifurcation, which creates the need for a method which is precise also in the advanced postbuckling regime. Comprehensive comparison to numerical results proves our method accurate both close to and far from bifurcation.

We are confident that the principle of the hyperbolic asymptotic method will prove applicable to a wide range of structures. Though the upper bound may not always be as easily obtained, the correct global behavior of the asymptotic trial functions can still be investigated and used through knowledge of the postbuckling equilibrium between or close to bounds, for example, the upper bound, a simple expansion of the lower bound close to bifurcation, the elastic solution, an expansion at infinity, etc.

2. Geometrically imperfect model column

2.1. *General concept.* When the amplitude of the imperfection approaches zero, the equilibrium path of the imperfect structure approaches the postbuckling equilibrium path of the perfect one. Therefore, if the postbuckling equilibrium of the perfect model column has been determined, the equilibrium path of the imperfect structure may be found from an asymptotic expansion in a characteristic imperfection amplitude, which for the Shanley–Hutchinson column is the initial rotation $\bar{\theta}$ mentioned in Section 1.2; see Figure 10. A closer investigation of Hutchinson's asymptotic expansion at the onset of elastic unloading may provide useful knowledge on which to base the expansion mentioned above.

2.1.1. *Hutchinson's asymptotic expansion at onset of elastic unloading.* The equilibrium equations of the imperfect model exhibit singular behavior when elastic unloading initiates, and solutions including linear elastic unloading cannot be extended into the (hypo-)elastic zone. Asymptotic expressions for $\widehat{\bar{\theta}}$, $\widehat{P}$ and $\widehat{u}$ are given by Hutchinson [1973a]:

$$\widehat{\bar{\theta}} = \widehat{\theta}_1 \bar{\theta}^{\frac{1}{2}} + O(\bar{\theta}), \qquad \widehat{P} = 1 + \widehat{p}_1 \bar{\theta}^{\frac{1}{2}} + O(\bar{\theta}), \qquad \widehat{u} = u_c + \widehat{u}_1 \bar{\theta}^{\frac{1}{2}} + O(\bar{\theta}) \tag{22}$$

where

$$\widehat{\theta}_1 = \left(\frac{\omega}{a_1^{pla} - a_1^{ela}} \right)^{\frac{1}{2}}, \quad \widehat{p}_1 = \left(2a_1^{ela} - a_1^{pla} \right) \left(\frac{\omega}{a_1^{pla} - a_1^{ela}} \right)^{\frac{1}{2}}, \quad \widehat{u}_1 = \frac{L}{3\tilde{L}} p_1^e.$$
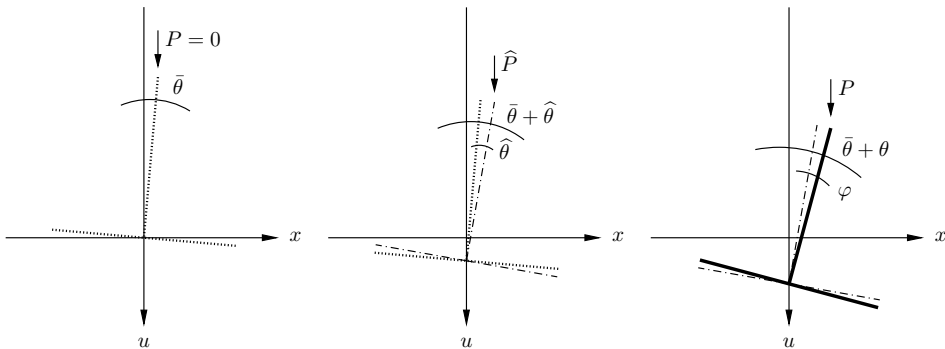

Figure 10. Definition of the kinematic variables θ, $\widehat{\theta}$, φ and u as well as various values of the load. The hat $\widehat{}$ indicates values at the onset of elastic unloading.

Here, a_1^{ela} and a_1^{pla} are the initial slopes of the elastic and plastic equilibrium paths of the geometrically perfect structure, respectively. The formula for ω is given by [Hutchinson 1974, Equation (2.52)][2]

$$\omega = \left(1 - \frac{LE_t^{c'}}{3E_t^c}\frac{L}{\tilde{L}}\right)^{-1}, \qquad a_1^{pla} = \frac{3\tilde{L}}{L}, \qquad a_1^{ela} = -\frac{3\omega k_1\tilde{L}}{2L}.$$

Note that Equation (22) gives the onset of elastic unloading for the imperfect column as the onset of elastic unloading for the perfect column at bifurcation plus additional asymptotic terms in the imperfection $\bar{\theta}$.

2.1.2. *Asymptotic expansion for the imperfect column in the plastic domain.* In order to utilize Hutchinson's asymptotic expansion of the onset of unloading as a bound, or boundary state, of an asymptotic expansion of the equilibrium of the imperfect column after unloading has initiated, our expansion must match Hutchinson's expansion at the onset of unloading. Therefore, the fundamental form of the asymptotic expansion for the geometrically imperfect structure is taken to be

$$\theta_{\text{imp}}(\bar{\theta}) = \theta_{\text{per}} + \Delta\theta_i = \theta_{\text{per}} + \theta_1\bar{\theta}^{\frac{1}{2}} + O(\bar{\theta}),$$

$$P_{\text{imp}}(\bar{\theta}) = P_{\text{per}} + \Delta P_i = P_{\text{per}} + p_1\bar{\theta}^{\frac{1}{2}} + O(\bar{\theta}), \qquad (23)$$

$$u_{\text{imp}}(\bar{\theta}) = u_{\text{per}} + \Delta u_i = u_{\text{per}} + u_1\bar{\theta}^{\frac{1}{2}} + O(\bar{\theta}).$$

For brevity only the dependence on $\bar{\theta}$ is indicated. Subscripts $_{\text{per}}$ and $_{\text{imp}}$ refer to equilibrium of the perfect and the imperfect structure, respectively.

When the perfect column starts unloading θ increases from 0, and boundary conditions for the asymptotic functions θ_1, p_1 and u_1 given by Equation (22) yield

$$\theta_1\Big|_{\theta_{\text{per}}=0} = \widehat{\theta}_1, \qquad p_1\Big|_{\theta_{\text{per}}=0} = \widehat{p}_1, \qquad u_1\Big|_{\theta_{\text{per}}=0} = \widehat{u}_1.$$

One of the functions, θ_1, p_1 or u_1, in Equation (23) may be chosen independently as long as the boundary conditions given above are fulfilled, and all equilibrium states of the imperfect structure states may be reached. Since $\theta_{\text{per}} \in [0; \infty[$ and $\theta_{\text{imp}} \in [\widehat{\theta}_1\bar{\theta}^{\frac{1}{2}} + O(\bar{\theta}); \infty[$ a valid, simple choice of independent variable is

$$\theta_{\text{imp}}(\bar{\theta}) = \theta_{\text{per}} + \widehat{\theta}_1\bar{\theta}^{\frac{1}{2}} + O(\bar{\theta}), \qquad (24)$$

which for a given imperfection is just a transformation of θ as demonstrated in Figure 11. Note that when $\theta_{\text{per}} \geq 0$ the solutions for the perfect and the imperfect column both lie in the plastic domain.

This asymptotic approach to the plastic imperfection analysis has some advantages which are not present in earlier expansions:

  (i) it proves to be fairly simple;

 (ii) the accuracy of the imperfection sensitivity analysis will be good even for large $\varphi \equiv \theta - \widehat{\theta}$ if the solution for the geometrically perfect structure is accurate;

(iii) it allows utilization of either a numerical or an asymptotic solution to the geometrically perfect column, which can be of great advantage since a numerical solution that is accurate even for large values of θ may be obtained for most structures.

---

[2]Hutchinson [1974] uses ρ instead of ω, but for consistency with Section 1, where ρ is used for another purpose, we use ω.
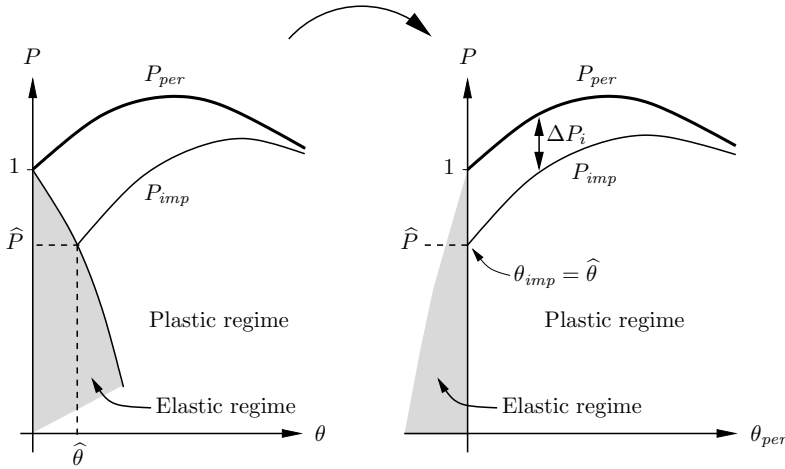
Figure 11. The asymptotic method for the imperfect structure.

2.2. *Asymptotic solution for the imperfect structure.* Equilibrium for the geometrically imperfect model column is controlled by Equations (9) and (10). These equations must be transformed in such a way that they depend only on θ_{per} and $\bar{\theta}$. Let a dot denote differentiation with respect to θ_{per}:

$$(\dot{\ }) \equiv \frac{\partial(\ )}{\partial\theta_{\mathrm{per}}}.$$

Since, according to Equation (24), $\dot{\theta}_{\mathrm{imp}} = 1$ holds everywhere, by insertion of Equations (23) and (24), Equations (9) and (10) are transformed into

$$\dot{P}_{\mathrm{imp}} = \int_{-\dot{u}_{\mathrm{imp}}}^{1} E_t^{\mathrm{imp}}(\dot{u}_{\mathrm{imp}} + x)dx + \int_{-1}^{-\dot{u}_{\mathrm{imp}}} E(\dot{u}_{\mathrm{imp}} + x)dx \tag{25}$$

and

$$\dot{P}_{\mathrm{imp}}(\theta_{\mathrm{per}} + \widehat{\theta}_1\bar{\theta}^{\frac{1}{2}} + O(\bar{\theta})) + P_{\mathrm{imp}} + (i+1)\,k_i\,(\theta_{\mathrm{per}} + \widehat{\theta}_1\bar{\theta}^{\frac{1}{2}} + O(\bar{\theta}))^i$$
$$= \int_{-\dot{u}_{\mathrm{imp}}}^{1} E_t^{\mathrm{imp}}(\dot{u}_{\mathrm{imp}} + x)\,x\,dx + \int_{-1}^{-\dot{u}_{\mathrm{imp}}} E(\dot{u}_{\mathrm{imp}} + x)\,x\,dx. \tag{26}$$

2.2.1. *Expansion of the tangent modulus.* In the vicinity of the solution for the geometrically perfect column the tangent modulus E_t can be given in terms of a Taylor expansion in the strain $\varepsilon_{\mathrm{imp}}$. For a given value of θ_{per} the expansion becomes:

$$E_t^{\mathrm{imp}}(\bar{\theta}, \theta_{\mathrm{per}}, x) = E_t^{\mathrm{per}}(\theta_{\mathrm{per}}, x) + (\varepsilon_{\mathrm{imp}} - \varepsilon_{\mathrm{per}})E_t^{\mathrm{per}'}(\theta_{\mathrm{per}}, x) + O((\varepsilon_{\mathrm{imp}} - \varepsilon_{\mathrm{per}})^2).$$

where prime $(')$ denotes differentiation with respect to ε, and the dependence of $\varepsilon_{\mathrm{imp}}$ and $\varepsilon_{\mathrm{per}}$ on the kinematic variables is not indicated. Insert ε as given by Equation (5) together with (23) and (24) and get:

$$E_t^{\mathrm{imp}}(\bar{\theta}, \theta_{\mathrm{per}}, x) = E_t^{\mathrm{per}}(\theta_{\mathrm{per}}, x) + \bar{\theta}^{\frac{1}{2}}\big(u_1(\theta_{\mathrm{per}}) + \widehat{\theta}_1 x\big)E_t^{\mathrm{per}'}(\theta_{\mathrm{per}}, x) + O(\bar{\theta}). \tag{27}$$

Notice that $E_t^{\text{per}}(\theta_{\text{per}}, x)$ and $E_t^{\text{per}'}(\theta_{\text{per}}, x)$ are known from the solution to the problem for the geometrically perfect structure alone.

2.2.2. *The governing equations.* Introduce E_t^{imp} given by Equation (27) and P_{imp} and u_{imp} given by Equation (23) in the equilibrium equations (25) and (26) for the imperfect column and obtain the equations of the asymptotic expansion in $\bar{\theta}$

$$\dot{P}_{\text{per}} + \dot{p}_1 \bar{\theta}^{\frac{1}{2}} = \int_{d_{\text{per}}}^{1} \left(E_t^{\text{per}} + \bar{\theta}^{\frac{1}{2}} (u_1 + \widehat{\theta}_1 x) E_t^{\text{per}'} \right) \left(\dot{u}_{\text{per}} + \dot{u}_1 \bar{\theta}^{\frac{1}{2}} + x \right) dx + \int_{-1}^{d_{\text{per}}} E \left(\dot{u}_{\text{per}} + \dot{u}_1 \bar{\theta}^{\frac{1}{2}} + x \right) dx$$

$$+ \int_{d_{\text{per}} - \dot{u}_1 \bar{\theta}^{\frac{1}{2}}}^{d_{\text{per}}} \left(E_t^{\text{per}} + \bar{\theta}^{\frac{1}{2}} (u_1 + \widehat{\theta}_1 x) E_t^{\text{per}'} \right) \left(\dot{u}_{\text{per}} + \dot{u}_1 \bar{\theta}^{\frac{1}{2}} + x \right) dx$$

$$+ \int_{d_{\text{per}}}^{d_{\text{per}} - \dot{u}_1 \bar{\theta}^{\frac{1}{2}}} E \left(\dot{u}_{\text{per}} + \dot{u}_1 \bar{\theta}^{\frac{1}{2}} + x \right) dx + O(\bar{\theta}) \quad (28)$$

and

$$\left(\dot{P}_{\text{per}} + \dot{p}_1 \bar{\theta}^{\frac{1}{2}} \right) \left(\theta_{\text{per}} + \widehat{\theta}_1 \bar{\theta}^{\frac{1}{2}} \right) + P_{\text{per}} + p_1 \bar{\theta}^{\frac{1}{2}} + (i+1) k_i \left(\theta_{\text{per}}^i + i \theta_{\text{per}}^{i-1} \widehat{\theta}_1 \bar{\theta}^{\frac{1}{2}} \right)$$

$$= \int_{d_{\text{per}}}^{1} \left(E_t^{\text{per}} + \bar{\theta}^{\frac{1}{2}} (u_1 + \widehat{\theta}_1 x) E_t^{\text{per}'} \right) \left(\dot{u}_{\text{per}} + \dot{u}_1 \bar{\theta}^{\frac{1}{2}} + x \right) x \, dx$$

$$+ \int_{-1}^{d_{\text{per}}} E \left(\dot{u}_{\text{per}} + \dot{u}_1 \bar{\theta}^{\frac{1}{2}} + x \right) x \, dx$$

$$+ \int_{d_{\text{per}} - \dot{u}_1 \bar{\theta}^{\frac{1}{2}}}^{d_{\text{per}}} \left(E_t^{\text{per}} + \bar{\theta}^{\frac{1}{2}} (u_1 + \widehat{\theta}_1 x) E_t^{\text{per}'} \right) \left(\dot{u}_{\text{per}} + \dot{u}_1 \bar{\theta}^{\frac{1}{2}} + x \right) x \, dx$$

$$+ \int_{d_{\text{per}}}^{d_{\text{per}} - \dot{u}_1 \bar{\theta}^{\frac{1}{2}}} E \left(\dot{u}_{\text{per}} + \dot{u}_1 \bar{\theta}^{\frac{1}{2}} + x \right) x \, dx + O(\bar{\theta}). \quad (29)$$

Eliminate the solution for the perfect structure, which is given by the terms of order zero in $\bar{\theta}$, and utilize that

$$\int_{c}^{c+\Delta} f(x) \left((x - c) - \Delta \right) dx = -\frac{1}{2} f(c) \Delta^2 + O(\Delta^3),$$

which proves that the last two integrals of both Equation (28) and Equation (29) are of order $O(\bar{\theta})$. The asymptotic equilibrium equations (28) and (29) therefore simplify to

$$\bar{\theta}^{\frac{1}{2}} \dot{p}_1 = \bar{\theta}^{\frac{1}{2}} \left(\dot{u}_1 f_1 + u_1 f_2 + \widehat{\theta}_1 f_3 \right) + O(\bar{\theta}),$$

$$\bar{\theta}^{\frac{1}{2}} \left(\dot{p}_1 \theta_{\text{per}} + p_1 \right) = \bar{\theta}^{\frac{1}{2}} \left(\dot{u}_1 f_4 + u_1 f_3 + \widehat{\theta}_1 f_5 \right) + O(\bar{\theta}),$$

(30)

where the functions $f_1, \ldots, f_5$ are associated with the solution for the geometrically perfect column and are:

$$f_1(\theta_{\text{per}}) = E(1 - \dot{u}_{\text{per}}(\theta_{\text{per}})) + \int_{d_{\text{per}}}^1 E_t^{\text{per}}(\theta_{\text{per}}, x)dx,$$

$$f_2(\theta_{\text{per}}) = \int_{d_{\text{per}}}^1 E_t^{\text{per}'}(\theta_{\text{per}}, x)(\dot{u}_{\text{per}}(\theta_{\text{per}}) + x)dx,$$

$$f_3(\theta_{\text{per}}) = \int_{d_{\text{per}}}^1 E_t^{\text{per}'}(\theta_{\text{per}}, x)(\dot{u}_{\text{per}}(\theta_{\text{per}}) + x)xdx, \tag{31}$$

$$f_4(\theta_{\text{per}}) = \frac{1}{2}E(\dot{u}_{\text{per}}^2(\theta_{\text{per}}) - 1) + \int_{d_{\text{per}}}^1 E_t^{\text{per}}(\theta_{\text{per}}, x)xdx,$$

$$f_5(\theta_{\text{per}}) = \int_{d_{\text{per}}}^1 E_t^{\text{per}'}(\theta_{\text{per}}, x)(\dot{u}_{\text{per}}(\theta_{\text{per}}) + x)x^2dx - \left(\dot{P}_{\text{per}} + (i+1)ik_i\theta_{\text{per}}^{i-1}\right).$$

In Appendix C, expressions for f_i, (C.5), which do not contain integrals, are computed but f_i may also be computed directly by inserting the stress-strain relation and the solution for the geometrically perfect structure.

2.2.3. *The first order imperfection sensitivity problem.* To establish the lowest order problem for the imperfect column gather terms of order $\bar{\theta}^{\frac{1}{2}}$ in the perturbed problems Equation (30) to get

$$\dot{p}_1 = \dot{u}_1 f_1 + u_1 f_2 + \widehat{\theta}_1 f_3, \qquad \dot{p}_1\theta_{\text{per}} + p_1 = \dot{u}_1 f_4 + u_1 f_3 + \widehat{\theta}_1 f_5. \tag{32}$$

The asymptotic procedure has reduced the problem of the equilibrium of the imperfect structure to be linear in that Equation (32) consists of two linear first order differential equations, which are easily solved by a numerical method using the boundary conditions at $\theta_{\text{per}} = 0$. A solution to Equation (32) yields the exact asymptotic equilibrium of the geometrically imperfect structure for *all* values of θ_{per}, including the particularly interesting exact asymptotic maximum load of the imperfect structure.

2.3. *Approximate determination of asymptotic functions.* To simplify the solution for the first order imperfection sensitivity problem Equation (32), we exploit the fact that p_1 and u_1 vary slowly with θ after the onset of elastic unloading to construct an approximate solution required to provide accurate estimates of the exact asymptotic maximum load. It was shown by van der Heijden [1979] that although the second derivatives of u and P are infinite only at initiating elastic unloading for the perfect structure, they become extremely large for small imperfections. This implies rapid variation of the derivatives of u and P which makes them unfit for asymptotic expansion close to initiating elastic unloading.

It will be shown in Section 2.4 that the exact asymptotic maximum load of the geometrically imperfect structure is found at $\theta_{\text{per}} = \theta_{\text{per}}^m$ where the maximum load of the perfect structure occurs. Here, superscript m indicates a quantity calculated at the maximum load. Expand p_1 and u_1 asymptotically around $\theta_{\text{per}} = \theta_{\text{per}}^m$ to determine the asymptotic behavior of the first order imperfection problem at maximum load of the imperfect structure.

Because the asymptotic equation (32) consists of two first order differential equations two boundary conditions are needed to fix our solution. The only directly accessible asymptotic boundary conditions for p_1 and u_1 are found at initiating elastic unloading where $p_1 = \widehat{p}_1$ and $u_1 = \widehat{u}_1$.

2.3.1. *Asymptotic expansion of the first order imperfection problem around maximum load.* Approximating polynomials for p_1 and u_1 around θ_{per}^m may be written as:

$$p_1 = p_1^1 + p_1^2 \Delta\theta + \frac{1}{2} p_1^3 (\Delta\theta)^2 + \cdots,$$

$$u_1 = u_1^1 + u_1^2 \Delta\theta + \frac{1}{2} u_1^3 (\Delta\theta)^2 + \cdots, \tag{33}$$

where $\Delta\theta = \theta_{\text{per}} - \theta_{\text{per}}^m$, $\Delta\theta \in \left[-\theta_{\text{per}}^m; 0\right]$ and the total asymptotic solution for the imperfect structure is

$$P_{\text{imp}} = P_{\text{per}} + \bar{\theta}^{\frac{1}{2}} \left(p_1^1 + p_1^2 \Delta\theta + \frac{1}{2} p_1^3 (\Delta\theta)^2 + \cdots \right) + O(\bar{\theta}),$$

$$u_{\text{imp}} = u_{\text{per}} + \bar{\theta}^{\frac{1}{2}} \left(u_1^1 + u_1^2 \Delta\theta + \frac{1}{2} u_1^3 (\Delta\theta)^2 + \cdots \right) + O(\bar{\theta}).$$

The lowest order imperfection problem is linear in both p_1 and u_1 and their derivatives. Hence, it follows that p_1^i and u_1^i may be given as linear functions of p_1^1 and u_1^1 when Equation (32) is expanded asymptotically around θ_{per}^m

$$f_i(\Delta\theta) = f_i^m + \Delta\theta \, \dot{f}_i^m + O(\Delta\theta^2). \tag{34}$$

The functions, f_i and $\dot{f}_i$, are given in Appendices C and D, respectively. The functions f_i^m and $\dot{f}_i^m$ are then found by inserting θ_{per}^m in Equation (31). Assume that f_i^m and $\dot{f}_i^m$ have been determined and insert Equations (33) and (34) in Equation (32) to get the asymptotic equations at the maximum load by gathering terms of the same order in $\Delta\theta$.

Zeroth order in $\Delta\theta$:

$$p_1^2 = u_1^2 f_1^m + u_1^1 f_2^m + \widehat{\theta}_1 f_3^m,$$

$$p_1^2 \theta_{\text{per}}^m + p_1^1 = u_1^2 f_4^m + u_1^1 f_3^m + \widehat{\theta}_1 f_5^m. \tag{35}$$

First order in $\Delta\theta$:

$$p_1^3 = u_1^3 f_1^m + u_1^2 (f_2^m + \dot{f}_1^m) + u_1^1 \dot{f}_2^m + \widehat{\theta}_1 \dot{f}_3^m,$$

$$p_1^3 \theta_{\text{per}}^m + 2 p_1^2 = u_1^3 f_4^m + u_1^2 (f_3^m + \dot{f}_4^m) + u_1^1 \dot{f}_3^m + \widehat{\theta}_1 \dot{f}_5^m. \tag{36}$$

This procedure may be extended to any order in $\Delta\theta$, but our experience shows that it is not necessary to go beyond the order used here, see below. Because the first order imperfection sensitivity problem Equation (32) is linear in p_1 and u_1, the above asymptotic equations of any order, Equations (35), (36), etc., are linear in the asymptotic coefficients p_1^i and u_1^i. As mentioned earlier the problem always entails two unknowns more than the number of equations because the first order imperfection sensitivity problem consists of two first order differential equations. To obtain the two additional equations required to determine p_1^i and u_1^i, assume that the asymptotic expansions of p_1 and u_1 around maximum furnish accurate results at initiating elastic unloading. This provides two boundary conditions at $\Delta\theta = -\theta_{\text{per}}^m$,

that is, $\theta_{\mathrm{per}} = 0$:

$$\widehat{p}_1 = p_1^1 + p_1^2(-\theta_{\mathrm{per}}^m) + \cdots + \frac{1}{n}p_1^{n+1}(-\theta_{\mathrm{per}}^m)^n,$$

$$\widehat{u}_1 = u_1^1 + u_1^2(-\theta_{\mathrm{per}}^m) + \cdots + \frac{1}{n}u_1^{n+1}(-\theta_{\mathrm{per}}^m)^n.$$

The asymptotic equations of order 0 to n, Equations (35), (36), etc., plus the general boundary conditions given above constitute $2(n+1)$ linear equations with $2(n+1)$ unknown asymptotic coefficients to determine the approximate asymptotic polynomials of degree n.

In practice it turns out that linear approximations yield good results, while parabolic approximations provide excellent accuracy for the maximum load because of the slow variation of p_1 and u_1. Thus, the problem of investigating imperfection sensitivity is reduced to solving 4 (linear approximation) or 6 (parabolic approximation) linear equations with 4 or 6 unknowns, respectively.

2.4. The maximum load. Only if the solution $p_1(\Delta\theta)$ is found exactly are we able to determine the maximum load asymptotically correct. On the other hand, if we have a good approximation of $p_1(\Delta\theta)$ near the maximum load of the perfect column, a good estimate of the asymptotic maximum load may be obtained. Close to the maximum load of the perfect structure, P_{per} may asymptotically be given as

$$P_{\mathrm{per}}(\Delta\theta) = P_{\mathrm{per}}^m + \frac{1}{2}\Delta\theta^2 \ddot{P}_{\mathrm{per}}^m + O(\Delta\theta^3),$$

because the first derivative $\dot{P}_{\mathrm{per}}^m$ of the load equilibrium for the perfect structure vanishes.

Expand P_{imp} in Equation (23) as

$$P_{\mathrm{imp}}(\Delta\theta) \approx P_{\mathrm{per}}^m + \frac{1}{2}\Delta\theta^2 \ddot{P}_{\mathrm{per}}^m + \bar{\theta}^{\frac{1}{2}}(p_1^1 + p_1^2\Delta\theta + \frac{1}{2}p_1^3\Delta\theta^2) + O(\bar{\theta}, \Delta\theta^3). \tag{37}$$

When the first order imperfection sensitivity problem Equation (32) is solved approximately by (33) p_1^i in (37) coincides with p_1^i in (33). In order for P_{imp} to attain a maximum (or minimum)

$$\Delta\theta_{\mathrm{imp}}^m = -\frac{p_1^2 \bar{\theta}^{\frac{1}{2}}}{\ddot{P}_{\mathrm{per}}^m} + O(\bar{\theta}),$$

which after insertion in Equation (37) furnishes the following approximate expression for the maximum load of the imperfect column

$$P_{\mathrm{imp}}^m = P_{\mathrm{per}}^m + p_1^1 \bar{\theta}^{\frac{1}{2}} + O(\bar{\theta}).$$

Note that, like in the elastic case, the maximum load-carrying capacity of the elastic-plastic imperfect structure compared to that of the perfect structure is controlled by only one parameter, namely p_1^1, the lowest order term in the approximation to p_1.

2.5. Asymptotic results and comparison. In Figures 12 and 13 the applicability of the approximate asymptotic method developed above is demonstrated by comparison with numerical results for two column geometries and two constitutive relations which entailed the least accurate asymptotic predictions in the studies by Hutchinson [1974] and by van der Heijden [1979] for the structures of Figures 13 and 12, respectively. The results of these studies were obtained by use of a Ramberg-Osgood type constitutive
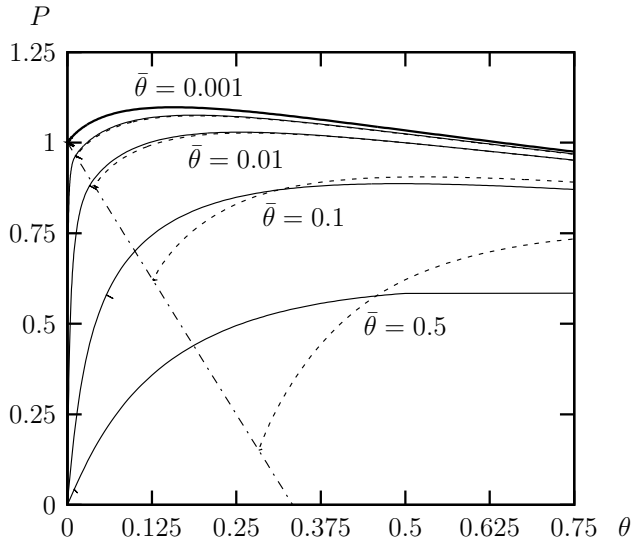
Figure 12. Comparison between numerical results and the approximate asymptotic method for $(n, \psi, s_c/s_y) = (3, 0.2, 1.4)$, $\rho = 3.0$. No kinematic nonlinearities, that is, $k_i = 0$. The dash-dot straight line indicates lowest order asymptotic prediction of initiation of linear elastic unloading. Here, the thick solid line represents perfect numerical, the thin solid line, imperfect numerical and the dashed line, asymptotic.

relation Equation (18). As shown in Section 1 the constitutive model Equation (17), which is better suited for our derivations, may predict a constitutive behavior very close to that of Equation (18) for the postbifurcation regime of the geometrically perfect column provided that the value of ρ is chosen appropriately. Both plots support the idea that our approximate asymptotic expansion for the imperfect column developed above does indeed approximate the exact solution very well in that our asymptotic curve almost coincides with both the shape and the values of the numerical curve for small imperfection amplitudes, that is, $\bar{\theta} \lesssim 0.001$.

In Figure 12 the maximum load-carrying capacity of the imperfect structure is approximated well even at the large imperfection $\bar{\theta} = 0.1$. However, for larger imperfection amplitudes our asymptotic expansion fails to predict the point of initial unloading accurately. For cases where the maximum load is located very close to initial unloading the maximum load is therefore not as well approximated for larger imperfections as it was in Figure 12. This is demonstrated by Figure 13 where for imperfections above approximately $\bar{\theta} = 0.1$ the numerical maximum load is obtained before the asymptotic method predicts initial unloading. Thus, for large imperfection amplitudes and maximum load close to initial unloading, our asymptotic method fails to predict the maximum load accurately because the point of initial unloading is poorly predicted by the nonlinear elastic asymptotic imperfection theory of the comparison model, as it was also pointed out by van der Heijden [1979].

In general, our asymptotic expansion to the lowest order of the equilibrium for the elastic-plastic imperfect column provides better estimates of maximum loads than its elastic counterpart. This is due to the fact that, in contrast to an elastic structure, a geometrically perfect plastic structure obtains its
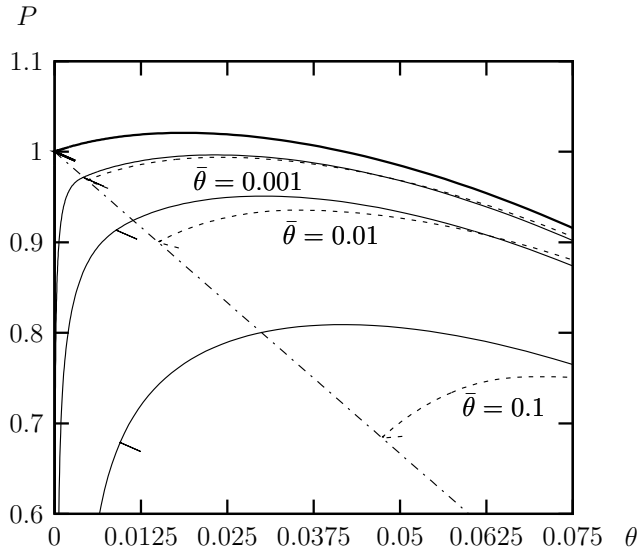
Figure 13. Comparison between numerical results and the approximate asymptotic method for $(n, \psi, s_c/s_y) = (10, 0.2, 1.2)$, $\rho = 25$. Kinematic nonlinearity given by $k_1/E = 1$. The dash-dot straight line indicates lowest order asymptotic prediction of initiation of linear elastic unloading. Here, the thick solid line represents Perfect numerical, the thin solid line, Imperfect numerical and the dashed line, Asymptotic.

maximum load at some finite distance from its lowest bifurcation load, where the asymptotic method provides better load estimates for an imperfect structure since it is further from the singular point of bifurcation. However, in order to obtain more accurate maximum load predictions for large imperfection amplitudes we need a better approximation by the nonlinear elastic asymptotic method of the point of initial unloading.

2.6. *Enhancement of the asymptotic solution.* Christensen and Byskov [2007a] establish a new expression, which is valid for the kinematically nonlinear equilibrium of an *elastic*, geometrically imperfect structure. It matches the traditional asymptotic expansion for an imperfect structure for buckling amplitudes $\theta \neq 0$, *and* for all imperfection amplitudes $\bar{\theta}$ it fulfills the boundary condition that $\theta = 0$ when the load $P = 0$. Christensen and Byskov [2007b] provide an example of the accuracy of this expression for the Euler column.

By comparison with numerical results it may be shown that, for relatively small θ, the kinematically nonlinear *elastic* equilibrium of an imperfect realization of the column shown in Figure 12 may be approximated in the following way

$$P = 1 - \frac{\rho\bar{\theta}}{\theta + \rho\bar{\theta}}, \qquad \frac{\partial P}{\partial \theta} = \frac{\rho\bar{\theta}}{(\theta + \rho\bar{\theta})^2}, \tag{38}$$

where the value of ρ depends on the parameters constitutive relation.

Because of extremely large derivatives of the elastic-plastic stress-strain relation relatively close to the critical stress, the preunloading path of the elastic-plastic imperfect column of Figure 13 is only approximated well when a higher order asymptotic expression for imperfection sensitivity is employed. Such an expansion has been developed by Christensen and Byskov [2007a].

To construct a simple enhancement of the solution for the imperfect structure, adopt the assumption that the nonlinear *elastic* path of the imperfect structure given by Equation (38) also describes the entire path of the *elastic-plastic* imperfect column well up till the asymptotic straight line emanating from the bifurcation point and separating the unloading and the nonunloading zone; see Figure 12. Let the enhanced asymptotic solution, which is in no way asymptotically more exact than the original one, be given as a higher order term of $\bar{\theta}$ added to the original solution

$$P_{\text{imp}}^e = P_{\text{per}} + p_1(\theta_{\text{per}})\bar{\theta}^{\frac{1}{2}} + \Delta p(\bar{\theta}), \qquad \theta_{\text{imp}}^e = \theta_{\text{per}} + \hat{\theta}_1\bar{\theta}^{\frac{1}{2}} + \Delta\theta(\bar{\theta}),$$

where superscript ^{e} indicates the enhanced asymptotic solution, and $\Delta p(\bar{\theta})$ and $\Delta\theta(\bar{\theta})$ are additions to the original asymptotic expansion which do not depend on θ_{per} and are both functions of order θ, leaving this expression asymptotically equivalent to the original asymptotic expansion. Note that

$$\left(\Delta p(\bar{\theta}), \Delta\theta(\bar{\theta})\right) \sim O(\bar{\theta}).$$

To fully fix Δp and $\Delta\theta$, use the boundary conditions such that

(i) the asymptotic solution passes through the point of initiating unloading as determined by the crossing between the straight boundary and the enhanced preunloading expression (38);

(ii) at the asymptotic straight boundary between no unloading and unloading, the derivative of the load P is continuous with respect to θ, as shown by van der Heijden [1979].

In Figure 14 the added precision of the enhanced approximate asymptotic method is demonstrated for the column of Figure 12, for which the previous asymptotic methods failed to provide reliable results for moderate and large imperfection levels. The asymptotic solution enhanced by better approximation of preunloading and the use of slope boundary conditions at initial asymptotic unloading for the column in question provides very close approximations to the numerical results both at maximum load and at initial unloading even at the large imperfection of $\bar{\theta} = 0.5$, which corresponds to an angle of $27°$.[3] Also, comparison with the original asymptotic expansion shows that the equilibrium prediction has been enhanced considerably, especially for the larger values of $\bar{\theta}$.

Conclusion. An asymptotic expression for the equilibrium of the imperfect realization of the Shanley–Hutchinson continuous model column is derived in the main body of this paper. The method hinges on the fact that for decreasing imperfections the equilibrium path of the imperfect structure approaches that of the perfect one, and that the expression for the path of the geometrically imperfect structure may be written as the postbuckling path of the perfect structure plus a small contribution which is expanded asymptotically to the lowest degree in the imperfection amplitude. The asymptotic coefficient associated with the lowest order imperfection amplitude is given by a linear, second order differential equation, which may be solved numerically. A simple polynomial approximation of the asymptotic coefficient function is derived based on its slow variation.

---

[3]For a model structure, such as the present one, the concept of large or small rotations is somewhat uncertain.
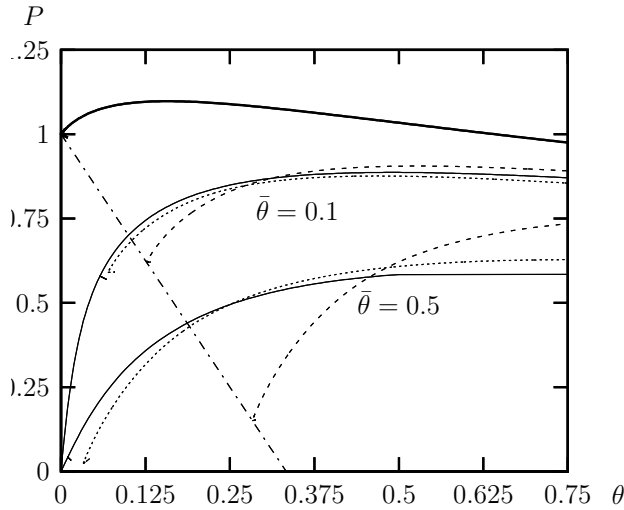
Figure 14. Comparison between numerical results, the approximate asymptotic method, and the enhanced approximate method applied to the column of Figure 12. The dash-dot straight line indicates lowest order asymptotic prediction of initiation of linear elastic unloading. The thick solid line represents the perfect, numerical, the thin solid line, imperfect, numerical, the dotted line, enhanced asymptotic and the dashed line, asymptotic results.

For a numerically determined postbuckling path, the approximate asymptotic equilibrium is determined for the column which in the study by van der Heijden [1979] proved to yield the most inaccurate estimates with his method. By our method, the approximation of the maximum load of the imperfect model column is excellent for small imperfections, and an asymptotic expansion which utilizes an enhanced approximation of initial unloading, provides very precise estimates of the entire equilibrium of the imperfect structure, even for large imperfections.

Appendix A: a study of Hutchinson's asymptotic method

Hutchinson [1973b; 1974] showed that $P_{\text{per}}(\theta)$ and $u_{\text{per}}(\theta)$ can be developed asymptotically in the spirit of Koiter's elastic theory [Koiter 1945] when extra terms containing fractional powers of θ are added. Hutchinson determined the form of the perturbation expansion for the Shanley–Hutchinson column to be

$$P = 1 + \Delta P = 1 + a_1\theta + a_2\theta^{\frac{3}{2}} + a_3\theta^2 + a_4\theta^{\frac{5}{2}} + a_5\theta^3 + a_6\theta^{\frac{7}{2}} + O(\theta^4), \tag{A.1}$$

$$u = u_c + \Delta u = u_c + b_1\theta + b_2\theta^{\frac{3}{2}} + b_3\theta^2 + b_4\theta^{\frac{5}{2}} + b_5\theta^3 + b_6\theta^{\frac{7}{2}} + O(\theta^4), \tag{A.2}$$

and calculated the first three constants of each expression. Here we determine two additional constants for both P and u. Knowing that elastic unloading starts at bifurcation we get

$$-d(\theta = 0) = \frac{\partial u}{\partial \theta}(\theta = 0) \Rightarrow b_1 = 1. \tag{A.3}$$

Expansion of the tangent modulus. In order to be able to carry out the integrations in Equation (9) and Equation (10) we expand E_t in Taylor series around $x = 0$. Use of ε given by Equation (5) provides $E_t = E_t(u) + (\theta x) E_t'(u) + \frac{1}{2}(\theta x)^2 E_t''(u) + \cdots$ where

$$( )' \equiv \frac{\partial ()}{\partial \varepsilon}.$$

Compute the integrals of the equilibrium equations (9) and (10) to transform them into ordinary differential equations:

$$\frac{\partial P}{\partial \theta} = \left(-\frac{1}{2} \left(\frac{\partial u}{\partial \theta} \right)^2 + \frac{\partial u}{\partial \theta} - \frac{1}{2} \right) E + \left(+\frac{1}{2} \left(\frac{\partial u}{\partial \theta} \right)^2 + \frac{\partial u}{\partial \theta} + \frac{1}{2} \right) E_t(u) + \left(-\frac{1}{6} \left(\frac{\partial u}{\partial \theta} \right)^3 + \frac{1}{2} \frac{\partial u}{\partial \theta} + \frac{1}{3} \right) \theta E_t'(u)$$

$$+ \left(+\frac{1}{12} \left(\frac{\partial u}{\partial \theta} \right)^4 + \frac{1}{3} \frac{\partial u}{\partial \theta} + \frac{1}{4} \right) \frac{\theta^2}{2} E_t''(u) + O(\theta^3),$$

and

$$\frac{\partial P}{\partial \theta} \theta + P + \frac{\partial K}{\partial \theta} = \left(+\frac{1}{6} \left(\frac{\partial u}{\partial \theta} \right)^3 - \frac{1}{2} \frac{\partial u}{\partial \theta} + \frac{1}{3} \right) E + \left(-\frac{1}{6} \left(\frac{\partial u}{\partial \theta} \right)^3 + \frac{1}{2} \frac{\partial u}{\partial \theta} + \frac{1}{3} \right) E_t(u)$$

$$+ \left(+\frac{1}{12} \left(\frac{\partial u}{\partial \theta} \right)^4 + \frac{1}{3} \frac{\partial u}{\partial \theta} + \frac{1}{4} \right) \theta E_t'(u)$$

$$+ \left(-\frac{1}{20} \left(\frac{\partial u}{\partial \theta} \right)^5 + \frac{1}{4} \frac{\partial u}{\partial \theta} + \frac{1}{5} \right) \frac{\theta^2}{2} E_t''(u) + O(\theta^3),$$

where

$$E_t^{(i)}(u) = E_t^{c(i)} + \Delta u E_t^{c(i+1)} + \frac{\Delta u^2}{2} E_t^{c(i+2)} + O(\theta^3),$$

with (i), $(i + 1)$ and $(i + 2)$ indicate the order of differentiation.

A.0.1. *The governing equations.* Employ the perturbation series for P and u given by Equations (A.1) and (A.2), respectively, and exploit the fact that $b_1 = 1$ (see Equation (A.3)) in order to establish the asymptotic equations:

$$0 = -a_1 - \frac{3}{2} a_2 \theta^{\frac{1}{2}} - 2a_3 \theta^1 - \frac{5}{2} a_4 \theta^{\frac{3}{2}} - 3a_5 \theta^2 + E \left(-\frac{9}{8} b_2^2 \theta^1 - 3b_2 b_3 \theta^{\frac{3}{2}} - (\frac{15}{4} b_2 b_4 + 2b_3^2) \theta^2 \right)$$

$$+ E_t^c \left(2 + 3b_2 \theta^{\frac{1}{2}} + (\frac{9}{8} b_2^2 + 4b_3) \theta^1 + (3b_2 b_3 + 5b_4) \theta^{\frac{3}{2}} + (\frac{15}{4} b_2 b_4 + 2b_3^2 + 6b_5) \theta^2 \right)$$

$$+ \left(\theta E_t^{c'} + \theta^{\frac{3}{2}} b_2 E_t^{c'} + \theta^2 (b_3 E_t^{c'} + \frac{1}{2} E_t^{c''}) \right) \left(2 + 3b_2 \theta^{\frac{1}{2}} + (\frac{9}{8} b_2^2 + 4b_3) \theta^1 \right)$$

$$+ \left(\theta E_t^{c'} + \theta^2 E_t^{c''} \right) \left(\frac{2}{3} - \frac{3}{8} b_2^2 \theta^1 \right) + \theta^2 \frac{1}{3} E_t^{c''} + O(\theta^{\frac{5}{2}}), \quad \text{(A.4)}$$

and

$$0 = +1 - 1 - 2a_1\theta - \tfrac{5}{2}a_2\theta^{\frac{3}{2}} - 3a_3\theta^2 - \tfrac{7}{2}a_4\theta^{\frac{5}{2}} - 2k_1\theta - 3k_2\theta^2$$

$$+\left(E - E_t^c\right)\left(\tfrac{9}{8}b_2^2\theta^1 + (3b_2b_3 + \tfrac{9}{16}b_2^3)\theta^{\frac{3}{2}} + (\tfrac{15}{4}b_2b_4 + \tfrac{9}{4}b_2^2b_3 + 2b_3^2)\theta^2\right.$$

$$\left.+(\tfrac{9}{2}b_2b_5 + 5b_3b_4 + \tfrac{45}{16}b_2^2b_4 + 3b_2b_3^2)\theta^{\frac{5}{2}}\right)$$

$$+\left(\theta E_t^{c'} + \theta^{\frac{3}{2}}b_2 E_t^{c'} + \theta^2(b_3 E_t^{c'} + \tfrac{1}{2}E_t^{c''}) + \theta^{\frac{5}{2}}(b_4 E_t^{c'} + b_2 E_t^{c''})\right)$$

$$\left(\tfrac{2}{3} - \tfrac{9}{8}b_2^2\theta^1 - (3b_2b_3 + \tfrac{9}{16}b_2^3)\theta^{\frac{3}{2}}\right)$$

$$+\left(\theta E_t^{c'} + \theta^2 E_t^{c''} + \theta^{\frac{5}{2}}b_2 E_t^{c''}\right)\left(\tfrac{2}{3} + b_2\theta^{\frac{1}{2}} + (\tfrac{4}{3}b_3 + \tfrac{9}{8}b_2^2)\theta^1 + (\tfrac{5}{3}b_4 + \tfrac{9}{8}b_2^3 + 3b_2b_3)\theta^{\frac{3}{2}}\right)$$

$$+\theta^2\tfrac{1}{5}E_t^{c''} + O(\theta^3). \quad \text{(A.5)}$$

Gather terms containing θ of the same order in Equations (A.4) and (A.5) and introduce the assumption that Equations (A.1) and (A.2) fulfill the equilibrium equations in a small area around $\theta = 0$. The polynomial identification theorem then gives us two sets of equations to determine the constants a_i and b_i. The first 5 terms in Equations (A.4) and (A.5) furnish

$$\theta^0: \quad a_1 = 3,$$

$$\theta^{\frac{1}{2}}: \quad a_2 = 3b_2,$$

$$\theta^1: \quad a_3 = \frac{1}{E - E_t^c}\left(2 - k_1 - E_t^{c'}\right) - 3 - k_1 + 2E_t^{c'}, \quad \text{(A.6)}$$

$$\theta^{\frac{3}{2}}: \quad a_4 = 3b_4 - \tfrac{6}{5}(E - E_t^c)b_2b_3 + 2E_t^{c'}b_2,$$

$$\theta^2: \quad a_5 = 3b_5 - \left(E - E_t^c\right)(\tfrac{5}{4}b_2b_4 + \tfrac{2}{3}b_3^2) + E_t^{c'}(2b_3 + b_2^2) + \tfrac{2}{3}E_t^{c''},$$

and

$$\theta^0: \quad 0 = 0,$$

$$\theta^{\frac{1}{2}}: \quad 0 = 0,$$

$$\theta^1: \quad b_2^2 = \frac{16}{9(E - E_t^c)}\left(3 + k_1 - \tfrac{2}{3}E_t^{c'}\right),$$

$$\theta^{\frac{3}{2}}: \quad b_3 = \frac{1}{3(E - E_t^c)}\left(2 - k_1 - E_t^{c'}\right), \quad \text{(A.7)}$$

$$\theta^2: \quad b_4 = \frac{4(a_3 + k_2)}{5(E - E_t^c)b_2} - \frac{8b_3^2}{15b_2} - \tfrac{3}{5}b_2b_3 - \frac{8E_t^{c'}b_3}{15(E - E_t^c)b_2} - \frac{8E_t^{c''}}{25(E - E_t^c)b_2},$$

$$\theta^{\frac{5}{2}}: \quad b_5 = \frac{7a_4}{9(E - E_t^c)b_2} - \frac{10b_3b_4}{9b_2} - \tfrac{5}{8}b_2b_4 - \tfrac{2}{3}b_3^2 - \frac{E_t^{c'}(-\tfrac{1}{8}b_2^3 + \tfrac{14}{27}b_4)}{(E - E_t^c)b_2} - \frac{14E_t^{c''}}{27(E - E_t^c)}.$$

These equations give us a_1 explicitly. The remaining constants a_i and b_i are found by alternately inserting the known quantities into Equations (A.6) and (A.7).

Appendix B: asymptotic expansion of ΔP^∞

In order to determine the coefficients for the new hyperbolic solution Equation (16), the ordinary polynomial expansion of ΔP_∞ is needed. Subtracting the asymptotic polynomial of P^∞ from that of the enhanced Hutchinson solution Equation (A.1) provides the desired polynomial.

The regular expansion of P^∞ (see Equation (20)) may be found as

$$P^\infty = 1 + 3\theta - (k_1 + 3\rho + 3)\theta^2 + \left(\tfrac{16}{5}\rho^2 + 3\rho + k_1 - k_2 + 3\right)\theta^3 + O(t^4).$$

Recall Equation (3) and realize that from Equation (17) we may find $\rho = -\dfrac{E_t^{c'}}{E_t^c}$, $\rho^2 = \dfrac{E_t^{c''}}{2E_t^c}$, then

$$P^\infty = 1 + 3\theta - (3 + k_1 - 2E_t^{c'})\theta^2 + \left(3 + k_1 - k_2 - 2E_t^{c'} + \tfrac{16}{15}E_t^{c''}\right)\theta^3 + O(t^4). \tag{B.1}$$

Introduce an asymptotic expansion of ΔP^∞:

$$\Delta P^\infty = a_1^\Delta \theta + a_2^\Delta \theta^{\frac{3}{2}} + a_3^\Delta \theta^2 + a_4^\Delta \theta^{\frac{5}{2}} + a_5^\Delta \theta^3 + O(\theta^{\frac{7}{2}}). \tag{B.2}$$

Recall the definition of ΔP^∞ (Equation (15)), the expansion for the total load P (see Equation (A.1)), utilize the results for a_j obtained in Equation (A.6), and compare the two ensuing expansions for ΔP^∞ to get the following expansions for a_j^Δ:

$$a_1^\Delta = 0, \qquad\qquad a_2^\Delta = a_2,$$

$$a_3^\Delta = a_3 + 3 + k_1 - 2E_t^{c'}, \qquad\qquad a_4^\Delta = a_4,$$

$$a_5^\Delta = a_5 - 3 - k_1 + k_2 + 2E_t^{c'} - \tfrac{16}{15}E_t^{c''}. \tag{B.3}$$

Appendix C: determination of f_i

We exploit the fact that the integrals of f_1 and f_2 can be computed directly when the solution for the geometrically perfect column is established

$$\int_{d_{\mathrm{per}}}^1 E_t^{\mathrm{per}} dx = \frac{1}{\theta_{\mathrm{per}}} \int_{x=d_{\mathrm{per}}}^{x=1} E_t^{\mathrm{per}} d\varepsilon_{\mathrm{per}} = \frac{s_{\mathrm{per}}\big|_{x=1} - s_{\mathrm{per}}\big|_{x=d}}{\theta_{\mathrm{per}}},$$

$$\int_{d_{\mathrm{per}}}^1 E_t^{\mathrm{per}'}(\dot{u}_{\mathrm{per}} + x) dx = \frac{1}{\theta_{\mathrm{per}}} \left(\left[E_t^{\mathrm{per}}(\dot{u}_{\mathrm{per}} + x)\right]_{d_{\mathrm{per}}}^1 - \int_{d_{\mathrm{per}}}^1 E_t^{\mathrm{per}} dx \right) \tag{C.1}$$

$$= \frac{E_t^{\mathrm{per}}\big|_{x=1}(\dot{u}_{\mathrm{per}} + 1)}{\theta_{\mathrm{per}}} - \frac{s_{\mathrm{per}}\big|_{x=1} - s_{\mathrm{per}}\big|_{x=d}}{\theta_{\mathrm{per}}^2},$$

which by insertion in Equation (31) gives us f_1 and f_2. The remaining functions are given as functions of f_1 and f_2 when we use the perfect equilibrium and its derivatives with respect to θ_{per}

$$P_{\mathrm{per}} = \int_{-1}^{d_{\mathrm{per}}} E(\dot{u}_{\mathrm{per}} + x) dx + \int_{d_{\mathrm{per}}}^1 E_t^{\mathrm{per}}(\dot{u}_{\mathrm{per}} + x) dx = \dot{u}_{\mathrm{per}} f_1 + f_4 \tag{C.2}$$

and

$$\ddot{P}_{\text{per}} = \int_{-1}^{d_{\text{per}}} E\ddot{u}_{\text{per}}dx + \int_{d_{\text{per}}}^{1} (E_t^{\text{per}}\ddot{u}_{\text{per}} + E_t^{\text{per}'}(\dot{u}_{\text{per}} + x)^2)dx = \ddot{u}_{\text{per}}f_1 + \dot{u}_{\text{per}}f_2 + f_3 \qquad \text{(C.3)}$$

and

$$\ddot{P}_{\text{per}}\theta_{\text{per}} + 2\dot{P}_{\text{per}} + (i+1)ik_i\theta_{\text{per}}^{i-1} = \int_{-1}^{d_{\text{per}}} E\ddot{u}_{\text{per}}xdx + \int_{d_{\text{per}}}^{1} (E_t^{\text{per}}\ddot{u}_{\text{per}} + E_t^{\text{per}'}(\dot{u}_{\text{per}} + x)^2)xdx$$

$$= \ddot{u}_{\text{per}}f_4 + \dot{u}_{\text{per}}f_3 + f_5 + \dot{P}_{\text{per}} + (i+1)ik_i\theta_{\text{per}}^{i-1}. \qquad \text{(C.4)}$$

The expressions for f_i can now be determined directly as functions of θ_{per} alone given by the solution for the geometrically perfect column problem. From Equations (C.1)–(C.4) and Equation (31), we get:

$$f_1 = E(L - \dot{u}_{\text{per}}) + \frac{s_{\text{per}}|_{x=1} - s_{\text{per}}|_{x=d}}{\theta_{\text{per}}}, \qquad f_2 = \frac{E_t^{\text{per}}|_{x=1}(\dot{u}_{\text{per}} + 1)}{\theta_{\text{per}}} - \frac{s_{\text{per}}|_{x=1} - s_{\text{per}}|_{x=d}}{\theta_{\text{per}}^2},$$

$$f_3 = \ddot{P}_{\text{per}} - \ddot{u}_{\text{per}}f_1 - \dot{u}_{\text{per}}f_2, \qquad f_4 = \dot{P}_{\text{per}} - \dot{u}_{\text{per}}f_1,$$

$$f_5 = \ddot{P}_{\text{per}}\theta_{\text{per}} + \dot{P}_{\text{per}} - \ddot{u}_{\text{per}}f_4 - \dot{u}_{\text{per}}f_3. \qquad \text{(C.5)}$$

Appendix D: determination of $\dot{f}_i$

While f_3, f_4 and f_5 are straight forward to differentiate given Equation (C.5), the derivatives of f_i with respect to θ_{per}, that is, $\dot{f}_1$ and $\dot{f}_2$ are slightly more difficult to calculate:

$$\dot{f}_1 = -\ddot{u}_{\text{per}}(E - E_t^{\text{per}}|_{x=d}) + \int_{d_{\text{per}}}^{1} E_t^{\text{per}'}(\dot{u}_{\text{per}} + x)dx = -\ddot{u}_{\text{per}}(E - E_t^{\text{per}}|_{x=d}) + f_2,$$

and

$$\dot{f}_2 = \int_{d_{\text{per}}}^{1} (E_t^{\text{per}''}(\dot{u}_{\text{per}} + x)^2 + \ddot{u}_{\text{per}}E_t^{\text{per}'})dx$$

$$= \frac{1}{\theta_{\text{per}}}\left(\left[E_t^{\text{per}'}(\dot{u}_{\text{per}} + x)^2\right]_{d_{\text{per}}}^{1} - \ddot{u}_{\text{per}}\left(\int_{d_{\text{per}}}^{1} E_t^{\text{per}'}2(\dot{u}_{\text{per}} + x)dx + E_t^{\text{per}}|_{x=d} - E_t^{\text{per}}|_{x=1}\right)\right)$$

$$= \frac{1}{\theta_{\text{per}}}\left(\ddot{u}_{\text{per}}\left(E_t^{\text{per}}|_{x=1} - E_t^{\text{per}}|_{x=d} - 2f_2\right) + E_t^{\text{per}'}|_{x=1}(\dot{u}_{\text{per}} + 1)^2\right).$$

Finally, differentiation provides the remaining $\dot{f}_i$

$$\dot{f}_3 = \dddot{P}_{\text{per}} - \dddot{u}_{\text{per}}f_1 - \ddot{u}_{\text{per}}(\dot{f}_1 + f_2) - \dot{u}_{\text{per}}\dot{f}_2,$$

$$\dot{f}_4 = \ddot{P}_{\text{per}} - \ddot{u}_{\text{per}}f_1 - \dot{u}_{\text{per}}\dot{f}_1,$$

$$\dot{f}_5 = \dddot{P}_{\text{per}}\theta_{\text{per}} + 2\ddot{P}_{\text{per}} - \dddot{u}_{\text{per}}f_4 - \ddot{u}_{\text{per}}(\dot{f}_4 + f_3) - \dot{u}_{\text{per}}\dot{f}_3.$$

References

[Byskov 1982–83] E. Byskov, "Plastic symmetry of Roorda's frame", *J. Struct. Mech.* **10**:3 (1982–83), 311–328.

[Christensen and Byskov 2007a] C. D. Christensen and E. Byskov, "Nonlinear elastic and kinematic asymptotic postbuckling and imperfection sensitivity", 2007. To be submitted.

[Christensen and Byskov 2007b] C. D. Christensen and E. Byskov, "Plastic stability and imperfection sensitivity of the Euler column", 2007. To be submitted.

[Duberg and Wilder 1952] J. E. Duberg and T. W. Wilder, "Inelastic column behavior", NACA Report NACA-TR-1072, 1952, Available at http://hdl.handle.net/2060/19930092117.

[Engesser 1889] F. Engesser, "Die knickfestigkeit gerader Stäbe", *Z. Arch. Ing. Vereins Hannover* **1.7** (1889), 35–455.

[van der Heijden 1979] A. van der Heijden, "A study of Hutchinson's plastic buckling model", *J. Mech. Phys. Solids* **27**:5-6 (1979), 441–464.

[Hill 1957] R. Hill, "Stability of rigid-plastic solids", *J. Mech. Phys. Solids* **6**:1 (1957), 1–8.

[Hutchinson 1972] J. W. Hutchinson, "On the postbuckling behavior of imperfection-sensitive structures in the plastic range", *J. Appl. Mech.* (*Trans. ASME*) **39** (1972), 155–162.

[Hutchinson 1973a] J. W. Hutchinson, "Imperfection-sensitivity in the plastic range", *J. Mech. Phys. Solids* **21**:3 (1973), 191–204.

[Hutchinson 1973b] J. W. Hutchinson, "Post-bifurcation behavior in the plastic range", *J. Mech. Phys. Solids* **21**:3 (1973), 163–190.

[Hutchinson 1974] J. W. Hutchinson, "Plastic buckling", *Advances in Applied Mechanics* **14** (1974), 67–144.

[Hutchinson and Budiansky 1976] J. W. Hutchinson and B. Budiansky, "Analytical and numerical study of the effects of initial imperfections on the inelastic buckling of a cruciform column", pp. 98–105 in *Buckling of structures: symposium* (Cambridge, MA), edited by B. Budiansky, Springer-Verlag, Berlin, 1976.

[Koiter 1945] W. T. Koiter, *The stability of elastic equilibrium (Dissertation,Delft University)*, H.J. Paris, Amsterdam, 1945. (in Dutch); also NASA TT-F10,833, (1967); also Air Force Flight Dynamics Laboratory, AFFDL-TR-70-25, (1970).

[Koiter 1966] W. Koiter, "Post-buckling analysis of a simple two-bar frame", in *Recent progress in applied mechanics: the Folke Odqvist volume*, edited by B. Broberg et al., Almqvist and Wiksell, Stockholm, 1966.

[Ming and Wenda 1990] S. X. Ming and L. Wenda, "Postbuckling and imperfection sensitivity analysis of structures in the plastic range, I: model analysis", *Thin Wall. Struct.* **10**:4 (1990), 263–275.

[Needleman and Tvergaard 1976] A. Needleman and V. Tvergaard, "An analysis of the imperfection sensitivity of square elastic-plastic plates under axial compression", *Int. J. Solids Struct.* **12**:3 (1976), 185–201.

[Roorda 1965] J. Roorda, "Stability of structures with small imperfections", *J. Eng. Mech. Div ASCE* **91** (1965), 87–95.

[Scherzinger and Triantafyllidis 1998] W. Scherzinger and N. Triantafyllidis, "Asymptotic analysis of stability for prismatic solids under axial loads", *J. Mech. Phys. Solids* **46**:6 (1998), 955–1007.

[Shanley 1947] F. R. Shanley, "Inelastic column theory", *J. Aeronaut. Sci.* **14** (1947), 261–267.

CLAUS DENCKER CHRISTENSEN: Claus.DenckerChristensen@nktflexibles.com
NKT Flexibles I/S, Priorparken 510, 2605 Brøndby, Denmark

ESBEN BYSKOV: eb@civil.aau.dk
Department of Civil Engineering, Aalborg University, Sohngaardsholmsvej 57, DK-9000 Aalborg, Denmark